図・本館

Functional analysis of Tim50, a novel subunit of the TIM23 complex that links mitochondrial protein translocation across the outer and inner membranes

タンパク質のミトコンドリア外膜透過と内膜透過を共役させる
TIM23 複合体の新規構成因子 Tim50 の機能解析

2004, Dr. of Science Thesis

Hayashi Yamamoto

山本　林

Department of Chemistry
Graduate School of Science
Nagoya University

名古屋大学図書

41370383

ACKNOWLEDGMENTS

I wish to express my greatest gratitude to Professor Toshiya Endo for continuous guidance and kind encouragement throughout the present study. I am deeply grateful to Dr. Shuh-ichi Nishikawa, Dr. Takashi Kanamori, and Dr. Masatoshi Esaki for valuable advice, discussion, and encouragement. I am also grateful to Dr. Tohru Yoshihisa for helpful advice and discussion.

I also express my thanks to Dr. Toshiyuki Miyata (National Cardiovascular Center) for peptide sequencing, Dr. Daisuke Kohda (Kyushu University) for mass spectrometry measurement, Dr. Elizabeth A. Craig (University of Wisconsin) for the yeast two-hybrid system, Dr. Injae Shin (Yonsei University) and Dr. Peter G. Schultz (The Scripps Research Institute) for the site-specific photocrosslinking system, Dr. Satoshi Harashima (Osaka University) for plasmid pCgHIS3, Dr. Yoh Wada (University of Tokyo) for plasmid pSK-3×HA, and Dr. Robert E. Jensen (Johns Hopkins University) for anti-PiC antibodies.

I also thank all the members of Prof. Endo's laboratory for helpful discussion.

Finally, I wish to express my sincere gratitude to my parents, Koh-ichi Yamamoto and Masako Yamamoto, for their understanding and continuous support.

Hayashi Yamamoto

February 22, 2004

CONTENTS

ABBREVIATIONS

BPA	DL-2-amino-5-(*p*-benzoylphenyl)pentanoic acid
BSA	bovine serum albumin
CBB	coomassie brilliant blue
CCCP	carbonyl cyanide *m*-chrolophenylhydrazone
Cytb_2	cytochrome b_2
DHFR	dihydrofolate reductase
DiSC$_3$(5)	3,3'-dipropylthiadicarbocyanine iodide
DTT	dithiothreitol
GMBS	*N*-γ-maleimidobutyryloxy-succinimide ester
HA	influenza virus hemagglutinin
HEPES	2-[4-(2-hydroxyethyl)-1-piperazinyl]ethanesulfonic acid
IgG	immunoglobulin G
IMS	intermembrane space
MALDI-TOF	matrix-assisted laser desorptoon ionization - time of flight
MBS	*m*-maleimidobenzoyl-*N*-hydroxysuccinimide ester
MOPS	3-(*N*-morpholino)propanesulfonic acid
MPP	matrix processing peptidase
MTX	methotrexate
NADH	β-nicotinamide adenine dinucleotide reduced form
NaDOC	sodium deoxycholate
NADPH	β-nicotinamide adenine dinucleotide phosphate reduced form
NMBz	4-(*N*-maleimido)benzophenone
ORF	open reading frame
PAGE	polyacrylamide gel electrophoresis
PCR	polymerase chain reaction
PMSF	phenylmethylsulfonyl fluoride
SDS	sodium dodecyl sulfate
TIM	translocator of the inner mitochondrial membrane
TOM	translocator of the outer mitochondrial membrane
Tris	tris(hydroxymethyl)aminomethane
$\Delta\Psi$	membrane potential

Chapter 1

General Introduction

1-1. Introduction

Mitochondria are essential organelles in eukaryotic cells and involved in many vital cellular processes including bioenergetics, apoptosis, and the metabolism of amino acids, lipids, and Fe/S clusters. Mitochondria are bounded by two biological membranes, the outer membrane and the inner membrane, that divide two aqueous compartments, the intermembrane space (IMS), between the outer and inner membranes, and the matrix, which is the innermost compartment enclosed by the inner membrane. Although mitochondria contain their own genomic systems and protein synthesis machineries in the matrix, only a few proteins are encoded by the mitochondrial genome. Thus, a large majority of ~1,000 different mitochondrial proteins are encoded by the nuclear genome, synthesized in the cytosol, and subsequently imported into mitochondria. Once within the mitochondria, the imported proteins are sorted to one of the four submitochondrial compartments. Therefore protein import into mitochondria is an essential process for mitochondrial biogenesis.

1-2. Mitochondrial targeting signals

Nuclear-encoded mitochondrial proteins essentially contain targeting information within themselves (1). Most mitochondrial proteins are synthesized as precursor proteins with N-terminal extensions, termed presequences, that contain sufficient targeting information directing precursor proteins into the matrix (2, 3). Presequences are typically 10-80 amino-acid residues in length and able to form positively charged amphiphilic α-helices. Once precursor proteins emerge in the matrix, the presequences are proteolytically cleaved off by the matrix processing peptidase (MPP) as they are not necessary for protein functions. On the other hand, some other mitochondrial proteins like polytopic inner-membrane proteins are synthesized without cleavable presequences and contain targeting information within their mature part as internal signals (4). In contrast to the presequences, the internal targeting signals are less characterized.

1-3. Translocator of the mitochondrial outer membrane

The complex processes of mitochondrial protein import are mediated by elaborate systems in mitochondria including the translocator complexes of the outer and inner membranes. The translocator of the outer mitochondrial membrane (TOM) mediates the entry of almost all nuclear-encoded mitochondrial proteins (5-8). In yeast *Saccharomyces cerevisiae*, the TOM complex consists of at least seven distinct proteins, Tom40, Tom22, Tom5, Tom6, Tom7, Tom20, and Tom70, with the number of name indicating the approximate molecular mass in kDa (Figure 1-1) (9). The integral membrane proteins, Tom20 and Tom70, which expose the large C-terminal domains to the cytosol, are primary import receptors for mitochondrial proteins (10-14). Tom20 mainly recognizes mitochondrial targeting signals present in the N-terminal presequences, whereas Tom70 preferentially interacts with proteins carrying internal targeting signals. Tom20 and Tom70 are peripheral subunits of the TOM complex. The membrane-embedded protein Tom40 constitutes a protein-conducting channel through which mitochondrial proteins traverse the outer membrane in unfolded conformations (15, 16). The TOM core complex additionally contains an integral membrane protein Tom22 and three small Tom proteins, Tom5, Tom6, and Tom7. The N-terminal domain of Tom22, which is exposed to the cytosol and enriched in negatively charged residues, may well complement the receptor function of Tom20 as a secondary receptor for presequence-containing precursor proteins by recognizing the positively charged face of the helical presequence (17). Tom22 also has a negatively charged C-terminal domain exposing to the IMS and contributes to a presequence-binding site, termed the *trans* site, on the IMS side of the outer membrane (18-20). One of the small Tom proteins, Tom5 mediates the protein transfer from the import receptors to the Tom40 channel (21). Other small Tom proteins, Tom6 and Tom7 play structural roles in the assembly and stability of the TOM complex. Tom6 promotes the assembly of the TOM complex, whereas Tom7 appears to have a destabilizing influence

on the TOM complex (22, 23). Among these TOM components, only Tom40 and Tom22 are essential for cell viability, confirming their importance for protein translocation across the outer membrane.

1-4. Translocator of the mitochondrial inner membrane

The mitochondrial inner membrane contains at least two structurally and functionally distinct translocator complexes, the TIM23 complex and the TIM22 complex (Figure 1-1). The TIM23 complex mainly mediates translocation of presequence-containing precursor proteins across the inner membrane, whereas the TIM22 complex is required for insertion of presequence-less polytopic membrane proteins into the inner membrane (5-8).

The TIM23 complex consists of two integral membrane proteins, Tim23 and Tim17, and a peripheral membrane protein Tim44. The C-terminal region of Tim23 is embedded in the inner membrane and constitutes a cation-selective protein-conducting channel, probably in cooperation with Tim17 (24, 25). Tim23 extends the N-terminal hydrophilic segment to the IMS, which functions as a receptor for presequences (24, 26), and the extreme N-terminal region of Tim23 is integrated into the outer membrane, indicating that Tim23 takes an unusual, dual-membrane-spanning topology (27). Tim44 is peripherally associated with both Tim23 and Tim17 on the matrix side and provides a membrane-associated anchor for the matrix molecular chaperone Ssc1p, a mitochondrial heat shock protein Hsp70 (mtHsp70), and its cochaperone Yge1p/Mge1p (28, 29). Ssc1p and Yge1p function as an import motor that drives protein translocation across the inner membrane (30-32). Recently, another component of the Tim44-Ssc1p-Yge1p motor complex, Tim14/Pam18, was identified (33, 34). Tim14/Pam18 is a DnaJ-like protein that is anchored to the inner membrane and stimulates the ATPase activity of Ssc1p (35). Unlike the TOM components, all the TIM23 components and the import motor components

are essential for cell viability.

Other translocator complex of the inner membrane, the TIM22 complex consists of a putative channel-forming protein Tim22 and accessory proteins, Tim54 and Tim18 (36-39). The TIM22 complex cooperates with a family of small Tim proteins, Tim8, Tim9, Tim10, Tim12, and Tim13 (40-43). Three hetero-oligomeric complexes of small Tim proteins have been described; the Tim9-Tim10 complex and the Tim8-Tim13 complex are soluble in the IMS, and the Tim9-Tim10-Tim12 complex is associated with the TIM22 complex on the IMS side. These small Tim complexes functionally link the TOM complex with the TIM22 complex, facilitating the transfer of presequence-less preproteins from the outlet of the TOM channel to the TIM22 complex.

1-5. Driving forces for mitochondrial protein import

Two energy sources are strictly required for import of presequence-containing precursor proteins into the matrix. The first energy source is the membrane potential ($\Delta\Psi$) across the inner membrane, which facilitates the translocation of the N-terminal parts of precursor proteins across the inner membrane through the TIM23 channel (44). The $\Delta\Psi$, negative on the matrix side, plays at least two roles in the precursor protein translocation; it directly activates the voltage-gated TIM23 channel (24, 25) and likely exerts an electrophoretic effect on the positively charged presequences toward the matrix (45, 46). The second energy source comes from the ATP hydrolysis in the matrix, which is utilized by the matrix molecular chaperone Ssc1p (44). The completion of the precursor protein translocation across the inner membrane is absolutely achieved by the ATP-dependent action of Ssc1p. In contrast to the protein translocation across the inner membrane, that across the outer membrane does not require the $\Delta\Psi$ and ATP, because there is no membrane potential across the outer membrane and no ATP-dependent chaperone in the IMS.

1-6. Missing link between the TOM complex and the TIM23 complex

The translocation of precursor proteins across the inner membrane appears to be tightly linked to their translocation across the outer membrane, because no soluble intermediates in the IMS can be observed (47, 48). Nevertheless, the TOM complex in the outer membrane and the TIM23 complex in the inner membrane are not permanently linked, but they can interact only in the presence of a translocating precursor protein to generate the TOM-TIM23-preprotein supercomplex (49-51). Therefore a precursor protein translocating through the TOM complex needs to engage the TIM23 complex in the boundary inner membrane, which is closely apposed to the outer membrane, to form a transient "translocation contact site" (52). Although the IMS domain of Tom22 and the N-terminal segment of Tim23 appear to facilitate the transfer of translocating precursor protein from the TOM complex to the TIM23 complex (20, 27, 53, 54), the molecular mechanism underlying the link of the translocation across the outer membrane and that across the inner membrane remains unclear.

In the present study, I identified Tim50, a new subunit of the TIM23 complex. Tim50 is an integral inner-membrane protein and exposes the large C-terminal domain to the IMS, which interacts with the N-terminal domain of Tim23. Tim50 is directly involved in translocation of presequence-containing precursor proteins, but not of presequence-less preproteins, across the inner membrane. Translocation intermediates lodged in the TOM channel is crosslinked to Tim50. On the basis of these observations, a possible role of Tim50 in linking the protein translocation across the outer and inner membranes will be discussed.

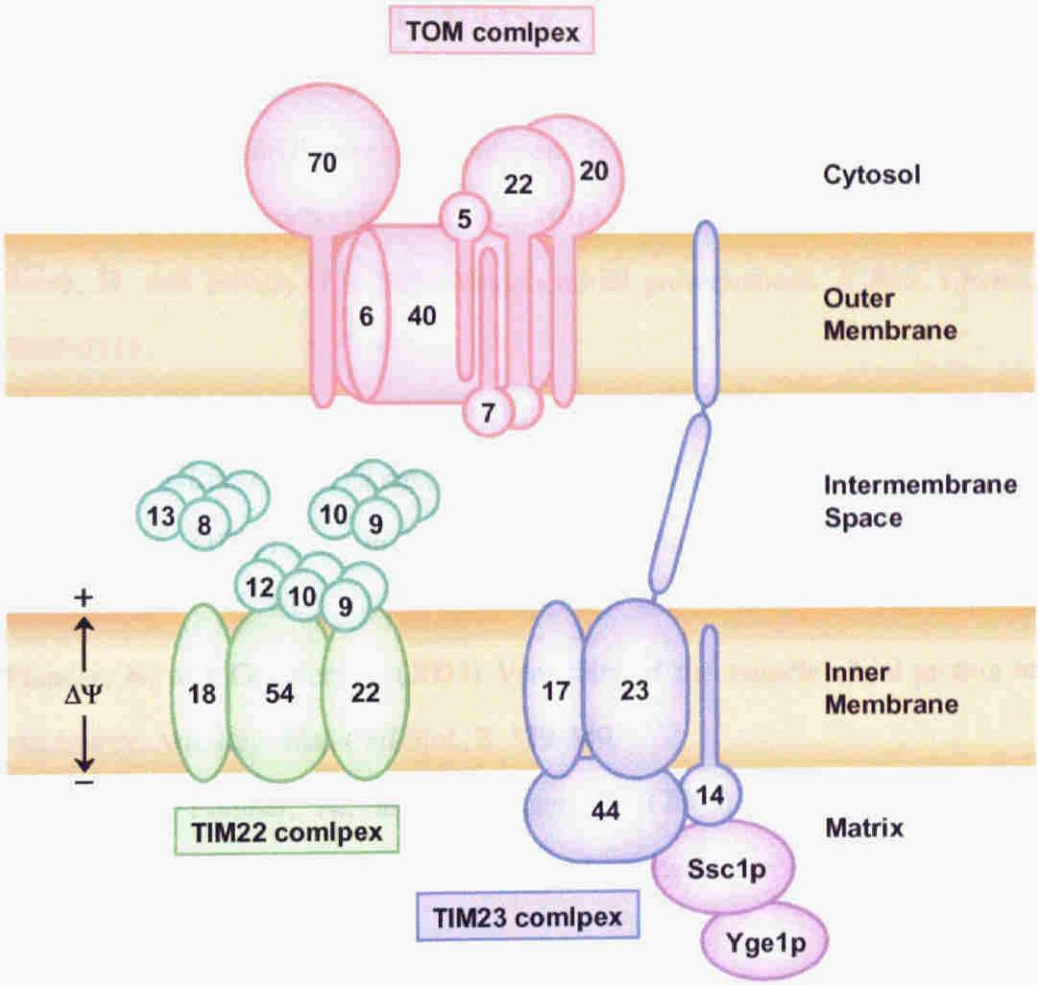

Figure 1-1. Translocator complexes of yeast mitochondria

In *Saccharomyces cerevisiae*, three types of mitochondrial translocator complexes are currently identified. The TOM complex (pink) in the outer membrane, and the TIM23 complex (blue) and the TIM22 complex (green) in the inner membrane are schematically shown. The subunits of these translocator complexes are named "Tom" for the TOM components or "Tim" for the TIM components with the numbers indicating their approximate molecular mass in kDa. Ssc1p and Yge1p (purple) in the matrix, which function as an import motor driving the translocation of presequence-containing precursor proteins across the inner membrane through the TIM23 complex, and small Tim complexes (light green) in the intermembrane space, which mediate the transfer of presequence-less preproteins from the outlet of the TOM complex to the TIM22 complex, are also shown. Import of presequence-containing precursor proteins into the matrix strictly requires two energy sources, the membrane potential ($\Delta\Psi$) across the inner membrane and the ATP hydrolysis in the matrix.

1-7. References

1) Schatz, G. and Dobberstein, B. (1996) Common principles of protein translocation across membranes. *Science*, **271**, 1519-1526.

2) Hurt, E. C., Pesold-Hurt, B., and Schatz, G. (1984) The amino-terminal region of an imported mitochondrial precursor polypeptide can direct cytoplasmic dihydrofolate reductase into the mitochondrial matrix. *EMBO J.*, **3**, 3149-3156.

3) Roise, D. and Schatz, G. (1988) Mitochondrial presequences. *J. Biol. Chem.*, **263**, 4509-4511.

4) Pfanner, N. and Neupert, W. (1987) Distinct steps in the import of ADP/ATP carrier into mitochondria. *J. Biol. Chem.*, **262**, 7528-7536.

5) Neupert, W. (1997) Protein import into mitochondria. *Annu. Rev. Biochem.*, **66**, 863-917.

6) Pfanner, N. and Geissler, A. (2001) Versatility of the mitochondrial protein import machinery. *Nat. Rev. Mol. Cell Biol.*, **2**, 339-349.

7) Rehling, P., Pfanner, N., and Meisinger, C. (2003) Insertion of hydrophobic membrane proteins into the inner mitochondrial membrane - a guided tour. *J. Mol. Biol.*, **326**, 639-657.

8) Endo, T., Yamamoto, H., and Esaki, M. (2003) Functional cooperation and separation of translocators in protein import into mitochondria, the double-membrane bounded organelles. *J. Cell Sci.*, **116**, 3259-3267.

9) Pfanner, N., Douglas, M. G., Endo, T., Hoogenraad, N. J., Jensen, R. E., Meijer, M., Neupert, W., Schatz, G., Schmitz, U. K., and Shore, G. C. (1996) Uniform nomenclature for the protein transport machinery of the mitochondrial membranes. *Trends Biochem. Sci.*, **21**, 51-52.

10) Söllner, T., Griffiths, G., Pfaller, R., Pfanner, N., and Neupert, W. (1989) MOM19, an import receptor for mitochondrial precursor proteins. *Cell*, **59**, 1061-1070.

11) Moczko, M., Gärtner, F., and Pfanner, N. (1993) The protein import receptor MOM19 of yeast mitochondria. *FEBS Lett.*, **326**, 251-254.

12) Ramage, L., Junne, T., Hahne, K., Lithgow, T., and Schatz, G. (1993) Functional cooperation of mitochondrial protein import receptors in yeast. *EMBO J.*, **12**, 4115-4123.

13) Hines, V., Brandt, A., Griffiths, G., Horstmann, H., Brütsch, H., and Schatz, G. (1990) Protein import into yeast mitochondria is accelerated by the outer membrane protein MAS70. *EMBO J.*, **9**, 3191-3200.

14) Steger, H. F., Söllner, T., Kiebler, M., Dietmeier, K. A., Pfaller, R., Trulzsch, K. S., Tropschug, M., Neupert, W., and Pfanner, N. (1990) Import of ADP/ATP carrier into mitochondria: two receptors act in parallel. *J. Cell Biol.*, **111**, 2353-2363.

15) Hill, K., Model, K., Ryan, M. T., Dietmeier, K., Martin, F., Wagner, R., and Pfanner, N. (1998) Tom40 forms the hydrophilic channel of the mitochondrial import pore for preproteins. *Nature*, **395**, 516-521.

16) Ahting, U., Thieffry, M., Engelhardt, H., Hegerl, R., Neupert, W., and Nussberger, S. (2001) Tom40, the pore-forming component of the protein-conducting TOM channel in the outer membrane of mitochondria. *J. Cell Biol.*, **153**, 1151-1160.

17) Brix, J., Dietmeier, K., and Pfanner, N. (1997) Differential recognition of preproteins by the purified cytosolic domains of the mitochondrial import receptors Tom20, Tom22, and Tom70. *J. Biol. Chem.*, **272**, 20730-20735.

18) Mayer, A., Neupert, W., and Lill, R. (1995) Mitochondrial protein import: reversible binding of the presequence at the trans side of the outer membrane drives partial translocation and unfolding. *Cell*, **80**, 127-137.

19) Rapaport, D., Neupert, W., and Lill, R. (1997) Mitochondrial protein import. Tom40 plays a major role in targeting and translocation of preproteins by forming a specific binding site for the presequence. *J. Biol. Chem.*, **272**, 18725-18731.

20) Kanamori, T., Nishikawa, S., Nakai, M., Shin, I., Schultz, P. G., and Endo, T. (1999) Uncoupling of transfer of the presequence and unfolding of the mature domain in precursor translocation across the mitochondrial outer membrane. *Proc. Natl. Acad. Sci. USA*, **96**, 3634-3639.

21) Dietmeier, K., Hönlinger, A., Bömer, U., Dekker, P. J. T., Eckerskorn, C., Lottspeich, F., Kübrich, M., and Pfanner, N. (1997) Tom5 functionally links mitochondrial preprotein receptors to the general import pore. *Nature*, **388**, 195-200.

22) Dekker, P. J. T., Ryan, M. T., Brix, J., Müller, H., Hönlinger, A., and Pfanner, N. (1998) Preprotein translocase of the outer mitochondrial membrane: molecular dissection and assembly of the general import pore complex. *Mol. Cell Biol.*, **18**, 6515-6524.

23) Hönlinger, A., Bömer, U., Alconada, A., Eckerskorn, C., Lottspeich, F., Dietmeier, K., and Pfanner, N. (1996) Tom7 modulates the dynamics of the mitochondrial outer membrane translocase and plays a pathway-related role in protein import. *EMBO J.*, **15**, 2125-2137.

24) Bauer, M. F., Sirrenberg, C., Neupert, W., and Brunner, M. (1996) Role of Tim23 as voltage sensor and presequence receptor in protein import into mitochondria. *Cell*, **87**, 33-41.

25) Truscott, K. N., Kovermann, P., Geissler, A., Merlin, A., Meijer, M., Driessen, A. J., Rassow, J., Pfanner, N., and Wagner, R. (2001) A presequence- and voltage-sensitive channel of the mitochondrial preprotein translocase formed by Tim23. *Nat. Struct. Biol.*, **8**, 1074-1082.

26) Komiya, T., Rospert, S., Koehler, C., Looser, R., Schatz, G., and Mihara, K. (1998) Interaction of mitochondrial targeting signals with acidic receptor domains along the protein import pathway: evidence for the 'acid chain' hypothesis. *EMBO J.*, **17**, 3886-3898.

27) Donzeau, M., Káldi, K., Adam, A., Paschen, S., Wanner, G., Guiard, B., Bauer, M. F., Neupert, W., and Brunner, M. (2000) Tim23 links the inner and outer mitochondrial membranes. *Cell*, **101**, 401-412.

28) Horst, M., Jeno, P., Kronidou, N. G., Bolliger, L., Oppliger, W., Scherer, P., Manning-Krieg, U., Jascur, T., and Schatz, G. (1993) Protein import into yeast mitochondria: the inner membrane import site protein ISP45 is the MPI1 gene product. *EMBO J.*, **12**, 3035-3041.

29) Blom, J., Kübrich, M., Rassow, J., Voos, W., Dekker, P. J. T., Maarse, A. C., Meijer, M., and Pfanner, N. (1993) The essential yeast protein MIM44 (encoded by MPI1) is involved in an early step of preprotein translocation across the mitochondrial inner membrane. *Mol. Cell Biol.*, **13**, 7364-7371.

30) Scherer, P. E., Krieg, U. C., Hwang, S. T., Vestweber, D., and Schatz, G. (1993) A precursor protein partly translocated into yeast mitochondria is bound to a 70 kd mitochondrial stress protein. *EMBO J.*, **9**, 4315-4322.

31) Kang, P. J., Ostermann, J., Shilling, J., Neupert, W., Craig, E. A., and Pfanner, N. (1990) Requirement for hsp70 in the mitochondrial matrix for translocation and folding of precursor proteins. *Nature*, **348**, 137-143.

32) Stuart, R. A., Cyr, D. M., Craig, E. A., and Neupert, W. (1994) Mitochondrial molecular chaperones: their role in protein translocation. *Trends Biochem. Sci.*, **19**, 87-92.

33) Mokranjac, D., Sichting, M., Neupert, W., and Hell, K. (2003) Tim14, a novel key component of the import motor of the TIM23 protein translocase of mitochondria. *EMBO J.*, **22**, 4945-4956.

34) Truscott, K. N., Voos, W., Frazier, A. E., Lind, M., Li, Y., Geissler, A., Dudek, J., Müller, H., Sickmann, A., Meyer, H. E., Meisinger, C., Guiard, B., Rehling, P., and Pfanner, N. (2003) A J-protein is an essential subunit of the presequence translocase-

associated protein import motor of mitochondria. *J. Cell Biol.*, **163**, 707-713.

35) D'Silva, P. D., Schilke, B., Walter, W., Andrew, A., and Craig, E. A. (2003) J protein cochaperone of the mitochondrial inner membrane required for protein import into the mitochondrial matrix. *Proc. Natl. Acad. Sci. USA*, **100**, 13839-13844.

36) Sirrenberg, C., Bauer, M. F., Guiard, B., Neupert, W., and Brunner, M. (1996) Import of carrier proteins into the mitochondrial inner membrane mediated by Tim22. *Nature*, **384**, 582-585.

37) Kerscher, O., Holder, J., Srinivasan, M., Leung, R. S., and Jensen, R. E. (1997) The Tim54p-Tim22p complex mediates insertion of proteins into the mitochondrial inner membrane. *J. Cell Biol.*, **139**, 1663-1675.

38) Kerscher, O., Sepuri, N. B., and Jensen, R. E. (2000) Tim18p is a new component of the Tim54p-Tim22p translocon in the mitochondrial inner membrane. *Mol. Biol. Cell*, **11**, 103-116.

39) Koehler, C. M., Murphy, M. P., Bally, N. A., Leuenberger, D., Oppliger, W., Dolfini, L., Junne, T., Schatz, G., and Or, E. (2000) Tim18p, a new subunit of the TIM22 complex that mediates insertion of imported proteins into the yeast mitochondrial inner membrane. *Mol. Cell. Biol.*, **20**, 1187-1193.

40) Curran, S. P., Leuenberger, D., Schmidt, E., and Koehler, C. M. (2002) The role of the Tim8p-Tim13p complex in a conserved import pathway for mitochondrial polytopic inner membrane proteins. *J. Cell Biol.*, **158**, 1017-1027.

41) Koehler, C. M., Merchant, S., Oppliger, W., Schmid, K., Jarosch, E., Dolfini, L., Junne, T., Schatz, G., and Tokatlidis, K. (1998) Tim9p, an essential partner subunit of Tim10p for the import of mitochondrial carrier proteins. *EMBO J.*, **17**, 6477-6486.

42) Sirrenberg, C., Endres, M., Fölsch, H., Stuart, R. A., Neupert, W., and Brunner, M. (1998) Carrier protein import into mitochondria mediated by the intermembrane proteins Tim10/Mrs11 and Tim12/Mrs5. *Nature*, **391**, 912-915.

43) Kurz, M., Martin, H., Rassow, J., Pfanner, N., and Ryan, M. T. (1999) Biogenesis of Tim proteins of the mitochondrial carrier import pathway: differential targeting mechanisms and crossing over with the main import pathway. *Mol. Biol. Cell.*, **10**, 2461-2474.

44) Herrmann, J. M. and Neupert, W. (2000) What fuels polypeptide translocation? An energetical view on mitochondrial protein sorting. *Biochim. Biophys. Acta*, **1459**, 331-338.

45) Martin, J., Mahlke, K., and Pfanner, N. (1991) Role of an energized inner membrane in mitochondrial protein import. $\Delta\Psi$ drives the movement of presequences. *J. Biol. Chem.*, **266**, 18051-18057.

46) Geissler, A., Krimmer, T., Bömer, U., Guiard, B., Rassow, J., and Pfanner, N. (2000) Membrane potential-driven protein import into mitochondria. The sorting sequence of cytochrome b_2 modulates the $\Delta\Psi$-dependence of translocation of the matrix-targeting sequence. *Mol. Biol. Cell*, **11**, 3977-3991.

47) Schleyer, M. and Neupert, W. (1985) Transport of proteins into mitochondria: translocational intermediates spanning contact sites between outer and inner membranes. *Cell*, **43**, 339-350.

48) Kanamori, T., Nishikawa, S., Shin, I., Schultz, P. G., and Endo, T. (1997) Probing the environment along the protein import pathways in yeast mitochondria by site-specific photocrosslinking. *Proc. Natl. Acad. Sci. USA*, **94**, 485-490.

49) Berthold, J., Bauer, M. F., Schneider, H.-C., Klaus, C., Dietmeier, K., Neupert, W., and Brunner, M. (1995) The MIM complex mediates preprotein translocation across the mitochondrial inner membrane and couples it to the mt-Hsp70/ATP driving system. *Cell*, **81**, 1085-1093.

50) Horst, M., Hilfiker-Rothenfluh, S., Oppliger, W., and Schatz, G. (1995) Dynamic interaction of the protein translocation systems in the inner and outer membranes of

yeast mitochondria. *EMBO J.*, **14**, 2293-2297.

51) Dekker, P. J. T., Martin, F., Maarse, A. C., Bömer, U., Müller, H., Guiard, B., Meijer, M., Rassow, J., and Pfanner, N. (1997) The Tim core complex defines the number of mitochondrial translocation contact sites and can hold arrested preproteins in the absence of matrix Hsp70-Tim44. *EMBO J.*, **16**, 5408-5019.

52) Pfanner, N., Rassow, J., van der Klei, I. J., and Neupert, W. (1992) A dynamic model of the mitochondrial protein import machinery. *Cell*, **68**, 999-1002.

53) Court, D. A., Nargang, F. E., Steiner, H., Hodges, R. S., Neupert, W., and Lill, R. (1996) Role of the intermembrane-space domain of the preprotein receptor Tom22 in protein import into mitochondria. *Mol. Cell. Biol.*, **16**, 4035-4042.

54) Moczko, M., Bömer, U., Kübrich, M., Zufall, N., Hönlinger, A., and Pfanner, N. (1997) The intermembrane space domain of mitochondrial Tom22 functions as a *trans* binding site for preproteins with N-terminal targeting sequences. *Mol. Cell. Biol.*, **17**, 6574-6584.

Chapter 2

Identification and Functional Analysis of Tim50

2-1. Introduction

Most mitochondrial proteins are synthesized in the cytosol as presequence-containing precursor proteins and traverse the mitochondrial outer and inner membranes through the TOM and TIM23 complexes, respectively. Although the translocation of precursor proteins across the outer membrane appears to be tightly linked to their translocation across the inner membrane, the direct interaction between the TOM and TIM23 components has not yet been observed. What mechanisms are underlying in the functional link between the TOM complex and the TIM23 complex?

Cytochrome b_2 (Cytb_2) is a major soluble protein in the IMS and synthesized as a precursor protein with an N-terminal bipartite presequence consisting of the matrix-targeting signal (residues 1-31) followed by the IMS-sorting signal (residues 32-80) (1). The Cytb_2 precursor is localized to the IMS by the following "stop-transfer" pathway (Figure 2-1) (2). Briefly, the N-terminal presequence part is translocated across the outer membrane through the TOM complex and transferred to the TIM23 complex. Then, the matrix-targeting signal part emerges in the matrix and is cleaved off by MPP, generating the processing-intermediate form (3). Simultaneously, further translocation across the inner membrane is arrested at the IMS-sorting signal part of the presequence and the processing-intermediate form is laterally released from the TIM23 complex, receives the second cleavage of the IMS-sorting signal by Imp1p in the IMS, and is converted to the mature form (4). Since this localization pathway of the Cytb_2 precursor is well characterized, Cytb_2 precursor fusion proteins have been employed as model substrates to analyze the mechanism of mitochondrial protein import.

The fusion protein pb_2(220)-DHFR contains the N-terminal 220 residues of the Cytb_2 precursor fused to mouse dihydrofolate reductase (DHFR) (Figure 2-2A), and is correctly localized to the IMS. When incubated with isolated yeast mitochondria in the presence of methotrexate (MTX), a high-affinity ligand for DHFR, pb_2(220)-DHFR is

complexed with MTX and arrested as a translocation intermediate spanning the outer membrane (5, 6), because the translocation across the mitochondrial membranes requires unfolding of the passenger domain. In this translocation intermediate, pb_2(220)-DHFR takes a topology in which the C-terminal DHFR domain remains outside the mitochondria whereas the N-terminal Cytb_2 precursor part has already traversed the outer membrane. Thus the N-terminus of pb_2(220)-DHFR is free in the IMS to form the mature form or is anchored to the inner membrane to form the processing-intermediate form (2). By using the technique of the site-specific photocrosslinking, Kanamori et al. (7) showed that the translocation intermediates of pb_2(220)-DHFR containing the unnatural amino acid with photoreactive crosslinker, DL-2-amino-5-(*p*-benzoylphenyl)pentanoic acid (BPA) (Figure 2-2B), at residues 94 or 114 were crosslinked with an unidentified mitochondrial protein to generate a ~95-kDa crosslinked product (Figure 2-3). In this crosslinked product, pb_2(220)-DHFR forms the processing-intermediate form that is anchored to the inner membrane with the crosslinking residue located just downstream of the IMS-sorting signal. Since the crosslinked partner could be a new component involved in protein translocation across the inner membrane, I decided to identify the crosslinked partner protein.

For this purpose, I prepared a recombinant pb_2(220)-DHFR-94C, a pb_2(220)-DHFR derivative harboring a unique cysteine residue at position 94, in large amounts from *E. coli* cells and modified it with 4-(*N*-maleimido)benzophenone (NMBz) to introduce the photoreactive benzophenone moiety to Cys-94. The NMBz-modified pb_2(220)-DHFR-94C yielded a crosslinked product of ~95 kDa and the crosslinked product was purified and subjected to tryptic digestion followed by mass spectrometry analysis. Thus I have identified a novel protein Tim50. I suggest that Tim50 is directly involved in the translocation of precursor proteins across the inner membrane and likely mediates the transfer of precursor proteins from the TOM complex to the TIM23 complex.

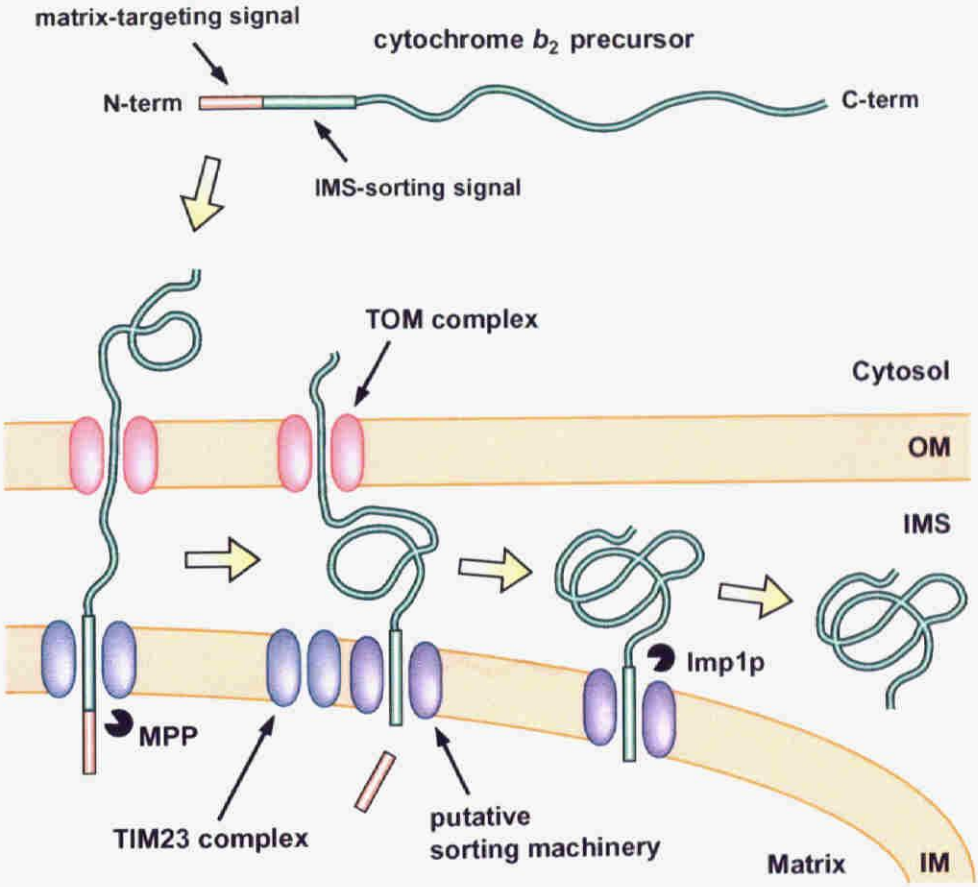

Figure 2-1. Localization pathway of cytochrome b_2 precursor into the intermembrane space

Cytochrome b_2 is synthesized in the cytosol as a precursor protein carrying an N-terminal bipartite presequence, in which the first part (matrix-targeting signal) directs the precursor protein to the matrix and is cleaved off by MPP in the matrix and the second part (IMS-sorting signal) mediates the sorting to the IMS and removed by Imp1p in the IMS. The cytochrome b_2 precursor is localized to the IMS according to the "stop-transfer" mechanism. OM, outer membrane; IMS, intermembrane space; IM, inner membrane.

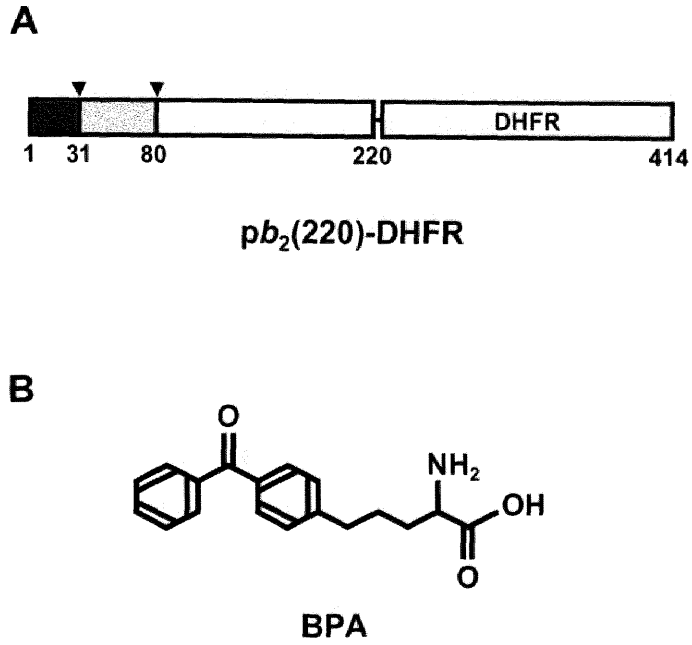

Figure 2-2. Schematic representation of the fusion protein pb_2(220)-DHFR and chemical structure of the unnatural amino acid BPA

(A) The fusion protein pb_2(220)-DHFR contains the first 220 residues of cytochrome b_2 precursor fused with a 7-residues linker fragment to mouse dihydrofolate reductase (DHFR). The first 80 residues of cytochrome b_2 precursor represents a bipartite presequence, in which residues 1-31 function as the matrix-targeting signal and residues 32-80 the IMS-sorting signal. Vertical arrowheads indicate the processing sites by MPP and Imp1p.

(B) Chemical structure of the unnatural amino acid with photoreactive crosslinker BPA. BPA, DL-2-amino-5-(*p*-benzoylphenyl)pentanoic acid.

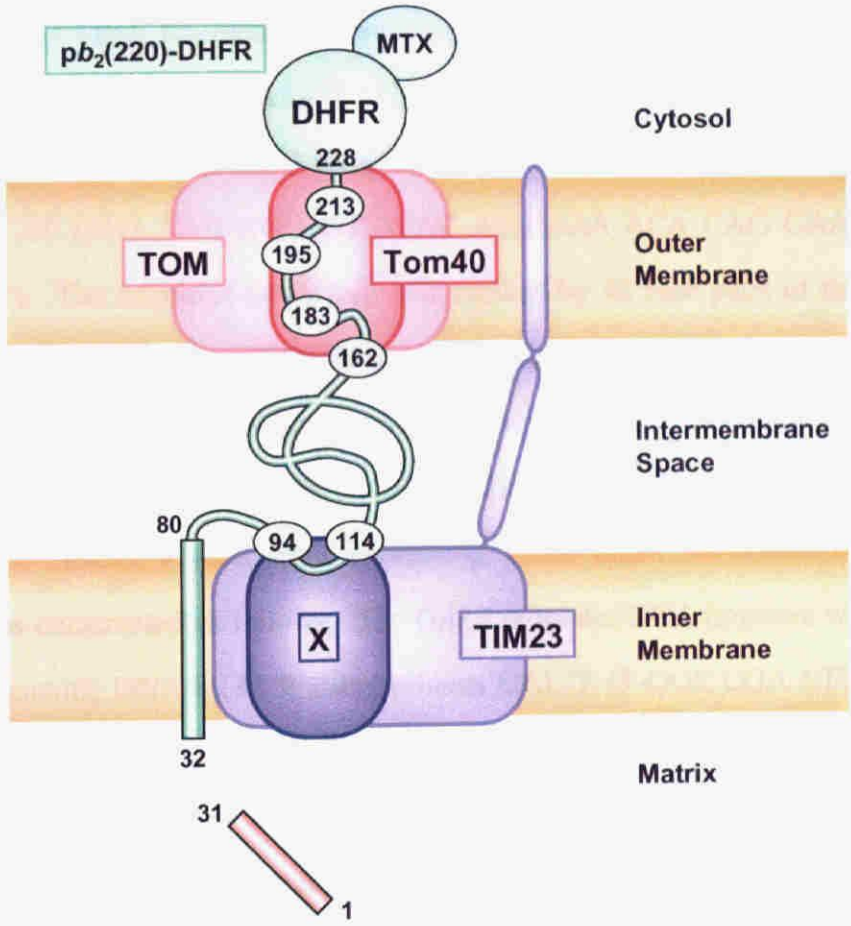

Figure 2-3. Translocation intermediate of pb_2(220)-DHFR containing BPA is crosslinked with the unidentified translocator component

Translocation intermediate of pb_2(220)-DHFR containing BPA was crosslinked with the unidentified translocator component (X) at residues 94 and 114 and with Tom40 at residues 162, 183, 195, and 213, in its processing-intermediate form anchored to the inner membrane. TOM, TOM complex; TIM23, TIM23 complex; DHFR, dihydrofolate reductase; MTX, methotrexate.

2-2. Materials and Methods

2-2-1. Yeast strains and plasmids

TIM50/tim50::CgHIS3, a yeast diploid strain carrying a complete null mutation in the chromosomal copy of *TIM50*, was constructed as follows. The *Candida glabrata HIS3* (*CgHIS3*) marker DNA fragment was amplified from plasmid pCgHIS3 (8) by PCR using primers Tim50CGF (5'-ATC ACA GCT AGA ATA AAC TTC CAA AAA TCA CCC GCT TGC AGT TGT AAA ACG ACG GCC AGT-3') and Tim50CGR (5'-ATA GAT ACG TAG ATA CAT GAG AAG AGG GTT TAC ATG AAA ACA CAG GAA ACA GCT ATG ACC-3'). The amplified DNA fragment, flanked by 40 base pairs of the sequences upstream and downstream of the *TIM50* gene, was transformed into yeast wild-type diploid strain W303-AB. The his^+ diploid transformants were isolated and confirmed by colony PCR analysis (9) to have one of the two copies of *TIM50* disrupted.

GAL7-TIM50, a yeast strain expressing Tim50 under the control of the *GAL7* promoter, was constructed as follows. The *GAL7* promoter DNA fragment was amplified from yeast genomic DNA by PCR using primers GAL7F (5'-GGC CGA ATT CAT ATA TTT TCT GTC ATT TTC-3') and GAL7R (5'-GGC CGG ATC CTT TTG AGG GAA TAT TCA ACT-3'), and the amplified DNA fragment was digested with *Eco*RI-*Bam*HI and inserted into pBluescript II SK- (Stratagene, La Jolla, CA, USA), resulting in pBS-GAL7. The *CgHIS3* marker DNA fragment was amplified from plasmid pCgHIS3 (8) by PCR using primers CgHIS3F (5'-CGC AAG CTT GGG TCT TCT GGA GCA CCG-3') and CgHIS3R (5'-GGC GAA TTC TGG CCC GAG TCA CCC AGC TC-3'), and the amplified DNA fragment was digested with *Hin*dIII-*Eco*RI and inserted into pBS-GAL7, resulting in pCgHIS3-GAL7. A DNA fragment containing the *CgHIS3* marker and the *GAL7* promoter was amplified from pCgHIS3-GAL7 by PCR using primers Tim50SOF (5'-CTG ATT TTT TGC TTT AGC ACA TCA CAG CTA GAA TAA ACT TCC AAA AAT CAC

CCG CTT GCA AAG CTT GGG TCT TCT GGA GC-3') and Tim50SOR (5'-TGG CAC AAC CCT AAG AGC CCT TGA ATT TAG TCT CAC CGA ATT TCT TAA AAT GGA CAG CAT TTT TGA GGG AAT ATT CAA CT-3') for subsequent integration into the chromosome upstream of the *TIM50* gene. The yeast wild-type haploid strain W303-1A was transformed with the amplified DNA fragment, and his^+ haploid transformants were isolated and confirmed by colony PCR analysis (9) to have the *TIM50* promoter replaced by the *GAL7* promoter.

TIM50-3HA, a yeast strain expressing the C-terminally 3HA-tagged Tim50 (Tim50-3HA) instead of wild-type Tim50, was constructed as follows. A DNA fragment containing the *TIM50* promoter and the *TIM50* gene was amplified from yeast genomic DNA by PCR using primers Tim50F (5'-GCC CTC GAG CCT CTT ACA TGT CTC AGG GC-3') and Tim50R (5'-GCC GGA TCC CGC GGA AAG TTG TGA GTA CG-3'), and the amplified DNA fragment was digested with *Xho*I-*Bam*HI and inserted into pBluescript II SK- (Stratagene, La Jolla, CA, USA), resulting in pBS-Tim50. A DNA fragment encoding triple-HA epitope, $(YPYDVPDYA)_3$, was amplified from plasmid pSK-3×HA (10) by PCR using phosphorylated primer Tim50HAF (5'-GAA GAA GAT TGC TGA ATC CAA ATA CCC ATA TGA CGT TCC AGA-3') and primer Tim50HAR (5'-AAG AGG GTT TAC ATG AAA ATT AAG CGT AGT CAG GTA CGT CGT AA-3'). The amplified DNA fragment was annealed to the uracil-containing single-strand DNA derived from pBS-Tim50 at the end of *TIM50* gene, and then extended and ligated, according to Kunkel et al. (11, 12), resulting in pBS-Tim50-3HA. The DNA fragment containing the *TIM50* promoter and the *TIM50-3HA* gene was prepared from pBS-Tim50-3HA and inserted into the *Xho*I-*Bam*HI site of the *CEN6-TRP1* plasmid pRS314 (13), resulting in pRS314-Tim50-3HA. The yeast diploid strain *TIM50/tim50::CgHIS3* was transformed with pRS314-Tim50-3HA and subjected to sporulation and tetrad analysis according to Rose et al. (14), and his^+trp^+ haploid cells, which express Tim50-3HA instead

of wild-type Tim50, were isolated.

TIM50&TIM50-3HA, a yeast strain expressing both wild-type Tim50 and Tim50-3HA was constructed as follows. The yeast haploid strain W303-1A was transformed with pRS314-Tim50-3HA and trp^+ haploid transformants were isolated.

TIM50-HIS6, a yeast strain expressing the C-terminally hexahistidine-tagged Tim50 (Tim50-His6) instead of wild-type Tim50 was constructed as follows. A DNA fragment containing the *TIM50* promoter and the *TIM50-HIS6* gene, was amplified from yeast genomic DNA by PCR using primers Tim50F and Tim50H6R (5'-GCC GGA TCC TTA GTG GTG GTG GTG GTG GTG TTT GGA TTC AGC AAT CTT CTT C-3'). The amplified DNA fragment was digested with *Xho*I-*Bam*HI and inserted into the *CEN6-URA3* plasmid pRS316 (13), resulting in pRS316-Tim50-His6. The yeast diploid strain *TIM50/tim50::CgHIS3* was transformed with pRS316-Tim50-His6 and subjected to sporulation and tetrad analysis according to Rose et al. (14), and his^+ura^+ haploid cells, which express Tim50-His6 instead of wild-type Tim50, were isolated.

pET-pb_2(220)CA-94C, a plasmid for expression of pb_2(220)-DHFR-94C in *E. coli* cells, was constructed as follows. The gene for pb_2(220)-DHFR-94C was derived from that for pb_2(220)-DHFR (7). The codons for Cys-16, Cys-105, Cys-174, Cys-234, and Ala-94 of the gene for pb_2(220)-DHFR were replaced by those for Ala-16, Ala-105, Ala-174, Ala-234, and Cys-94, according to Kunkel et al. (11, 12), and the resultant gene encoding pb_2(220)-DHFR-94C was digested with *Nde*I-*Xho*I and inserted into pET-21a(+) (Novagen, Darmstadt, Germany).

pET-Tim50(242-476), a plasmid for expression of the C-terminal segment (residues 242-476) of Tim50 in *E. coli* cells, was constructed by PCR using primers 242-Met (5'-CCA ACC ATA TGA TGT ACT CTG AC-3') and Lys-476 (5'-GGG TTT ACA TGA CTC GAG TTT GGA TTC AGC-3'). The amplified DNA fragment was digested with *Nde*I-*Xho*I and inserted into pET-21a(+) (Novagen, Darmstadt, Germany).

pRS314-Tim50, a plasmid for expression of Tim50 in yeast cells under the control of its own promoter, was constructed as follows. A DNA fragment containing the *TIM50* promoter and the *TIM50* gene was prepared from pBS-Tim50 and inserted into the *Xho*I-*Bam*HI site of the *CEN6-TRP1* plasmid pRS314 (13).

pGEM-Tim50, a plasmid for *in vitro* translation of the Tim50 precursor under the control of the SP6 promoter, was constructed by PCR using primers Tim50TTF (5'-GCC GAA TTC TAA ACT TCC AAA AAT CAC CC-3') and Tim50TTR (5'-CGG AAG CTT GTA GAT ACA TGA GAA GAG GG-3'). The amplified DNA fragment was digested with *Eco*RI-*Hin*dIII and inserted into pGEM-4Z (Promega, Madison, WI, USA).

For yeast two-hybrid analysis, a plasmid for expression of the IMS domain (residues 133-476) of Tim50 fused to the Gal4p activator domain and those for expression of residues 1-50, residues 51-96, and residues 1-96 of Tim23 fused to the Gal4p DNA binding domain were constructed by PCR using primers Tim50(133-) (5'-GGC GAA TTC AGG GAT TGG GAG CC-3') and Tim50(-476) (5'-GCC GGA TCC TTA TTT GGA TTC AGC-3'), Tim23(1-) (5'-GGC GAA TTC ATG TCG TGG CTT TTT GG-3') and Tim23(-50) (5'-GCC GGA TCC TTA TCC ACC AGG ACC TG-3'), Tim23(51-) (5'-GGC GAA TTC ATG CAT GTC GAC ACC GC-3') and Tim23(-96) (5'-GCC GGA TCC TTA GTC ATC GGT CCA CCC-3'), and Tim23(1-) and Tim23(-96), respectively. The amplified DNA fragments were digested with *Eco*RI-*Bam*HI and inserted into the *2μ-LEU2* plasmid pGAD-C1 (15) and the *2μ-URA3* plasmid pGBDU-C1 (15), respectively.

Yeast strains were grown in YPD (1% yeast extract, 2% polypeptone, 2% glucose), YPGal (1% yeast extract, 2% polypeptone, 2% galactose), and SD (0.67% yeast nitrogen base without amino acids, 2% glucose) supplemented with nucleotides and amino acids according to Rose et al. (14).

2-2-2. Identification of Tim50

Mitochondria were isolated from yeast wild-type strain D273-10B according to Daum et al. (16). The fusion protein pb_2(220)-DHFR-94C expressed in *E. coli* BL21(DE3) cells from plasmid pET-pb_2(220)CA-94C was purified as an inclusion body, solubilized with 8 M urea in 20 mM Tris-HCl pH 7.5, 50 mM KCl, 2 mM EDTA, and 0.2 mM DTT, and incubated with 2 mM 4-(*N*-maleimido)benzophenone (NMBz; Sigma-Aldrich, St. Louis, MO, USA) for 60 min on ice. After quenching the reaction by addition of 20 mM DTT, the NMBz-modified pb_2(220)-DHFR-94C was diluted 20-fold in 250 mM sucrose, 10 mM MOPS-KOH pH 7.2, 80 mM KCl, 2 mM KPi, 5 mM DTT, 5 mM $MgCl_2$, 2 mM ATP, 1% BSA, 10 μM MTX, and 1 mM NADPH, and incubated for 15 min on ice. Then, the reaction mixture received 2 mM NADH, and was incubated with the mitochondria (0.5 mg/ml proteins) for 20 min at 30°C to form a translocation intermediate. Then, the mitochondria were reisolated, suspended in 250 mM sucrose, 10 mM MOPS-KOH pH 7.2, 80 mM KCl, and 10 μM MTX, and subjected to UV irradiation with 365-nm UV lamp (15W, CSL-15A; Cosmo Bio, Tokyo, Japan) for 10 min on ice. The mitochondria were recovered and solubilized with HBR buffer (6 M urea, 50 mM Tris-HCl pH 7.9, 250 mM NaCl) containing 20 mM imidazole, 1% Triton X-100, and 1 mM PMSF, followed by clarifying centrifugation at 100,000 × *g* for 30 min at 4°C. The supernatants were incubated with His-Bind resin (Novagen, Darmstadt, Germany) for 12 hr at 4°C with gentle mixing. Then the resin was washed once with HBR buffer containing 20 mM imidazole and 1% Triton X-100, and washed twice with HBR buffer containing 20 mM imidazole. The bound proteins were eluted with HBR buffer containing 100 mM imidazole and subjected to SDS-PAGE and CBB R-250 staining. The CBB-stained 95-kDa crosslinked product was excised from the gel and prepared for mass spectrometry analysis (17). The molecular mass information of the tryptic peptides was obtained with a MALDI-TOF mass spectrometer Voyager Elite (PerSeptive Biosystems, Foster City, CA, USA). The abundant

ions in the MALDI spectra were calibrated with the internal control and used for database searches using the software PeptideSearch (developed at the EMBL Bioanalytical Research Group at Heidelberg, Germany; http://www.mann.embl-heidelberg.de/GroupPages/PageLink/peptidesearchpage.html), and the open reading frame *YPL063w* was identified by the matching of four ions, 1425.46 m/z, 1665.21 m/z, 1980.38 m/z, and 5559.57 m/z, corresponding to residues 393-404 (1426.6116 Da), residues 323-336 (1665.9696 Da), residues 372-392 (1980.2022 Da), and residues 164-210 (5559.4004 Da) of Tim50, respectively. The sequence coverage was 21.9%.

2-2-3. Antibodies against Tim50 and others

The C-terminal segment (residues 242-476) of Tim50 expressed in *E. coli* BL21(DE3) cells from plasmid pET-Tim50(242-476) was purified as an inclusion body and used for immunizing rabbits for obtaining anti-Tim50 antibodies (arbitrary rabbit numbers; 99-5 and 99-6). The mouse monoclonal antibody against the HA epitope (16B12) was purchased from Covance (Princeton, NJ, USA). The Cy5-conjugated goat anti-rabbit IgG antibody was purchased from Amersham Biosciences (Piscataway, NJ, USA). The specific IgGs for import inhibition were purified using Protein A Sepharose 4FF (Amersham Biosciences, Piscataway, NJ, USA) as follows. The antisera containing specific antibodies were incubated with Protein A Sepharose 4FF in 100 mM Tris-HCl pH 8.0 for 2 hr at room temperature with gentle mixing, and the bound IgGs were eluted with 0.1 M glycine-HCl pH 2.5, mixed with a 1/10 volume of 1 M Tris-HCl pH 8.0, and dialyzed against 20 mM Tris-HCl pH 7.2 and 80 mM KCl.

2-2-4. Immunofluorescence microscopy

Immunofluorescent staining of yeast cells was performed according to Kawai et al. (18) with minor modifications. Incubation with the primary and the secondary antibodies

was performed as follows; 1:500 dilution of rabbit anti-Tim50 polyclonal antisera and 1:500 dilution of mouse anti-porin monoclonal antibody (16G9-E6; Molecular Probes, Eugene, OR, USA) followed by 1:500 dilution of rhodamine-conjugated goat anti-rabbit IgG antibody (Valeant Pharmaceuticals International, Costa Mesa, CA, USA) and 1:500 dilution of alexa488-conjugated goat anti-mouse IgG antibody (Molecular Probes, Eugene, OR, USA), respectively.

2-2-5. Generation of mitoplasts and extraction of membrane proteins

For generation of mitoplasts, mitochondria were diluted 10-fold with 10 mM MOPS-KOH pH 7.2 and incubated for 20 min on ice. For alkaline extraction of peripheral membrane proteins, mitochondria were incubated with 0.1 M Na_2CO_3 at pH 11.5 for 30 min on ice, and then centrifuged at 100,000 × *g* for 30 min at 4°C. For extraction of integral membrane proteins with Triton X-100, mitochondria were incubated with 1% Triton X-100 in 250 mM sucrose, 10 mM MOPS-KOH pH 7.2, and 80 mM KCl for 30 min on ice, and then centrifuged at 100,000 × *g* for 30 min at 4°C. The samples were precipitated with 15% TCA and 0.05% NaDOC, and subjected to SDS-PAGE and immunoblotting followed by analyzing with a Storm 860 image analyzer (Amersham Biosciences, Piscataway, NJ, USA).

2-2-6. *In vitro* import into mitochondria

Mitochondria were isolated from yeast strains, D273-10B, W303-1A, and GAL7-TIM50 (16). Radiolabeled precursor proteins were synthesized in rabbit reticulocyte lysates by *in vitro* coupled transcription/translation system (19-21) in the presence of 0.02 MBq/μl [^{35}S]-methionine (Tran^{35}S-label; Valeant Pharmaceuticals International, Costa Mesa, CA, USA). Import reactions were performed by incubation of the translation products with isolated yeast mitochondria in Import buffer (250 mM sucrose, 10 mM MOPS-KOH pH 7.2, 80 mM KCl, 2 mM KPi, 2 mM methionine, 5 mM

DTT, 5 mM $MgCl_2$, 2 mM ATP, 2 mM NADH, 1% BSA) for 20 min at 30°C, except otherwise stated. The import reaction was stopped by addition of 10 μg/ml valinomycin. Protease treatment was performed, except otherwise stated, by incubating the mitochondria or mitoplasts with 100 μg/ml proteinase K for 20 min on ice, which was inactivated by subsequent addition of 1 mM PMSF. The samples were analyzed by SDS-PAGE and radioimaging with a Storm 860 image analyzer (Amersham Biosciences, Piscataway, NJ, USA). For generation of mitoplasts, mitochondria were diluted 10-fold with 10 mM MOPS-KOH pH 7.2 and incubated for 20 min on ice. For dissipation of $\Delta\Psi$, mitochondria were preincubated with 10 μg/ml valinomycin for 5 min on ice. For inactivation of MPP, mitochondria were preincubated with 1 mM *o*-phenanthroline and 5 mM EDTA in Import buffer without $MgCl_2$ for 3 min at 23°C.

To prepare the C-terminally truncated Tim50 precursors with defined lengths, plasmid pGEM-Tim50 for *in vitro* translation of the Tim50 precursor was digested with restriction enzymes, *Bst*PI, *Eco*T22I, *Nco*I, and *Fba*I, to yield truncated genes coding for the first 225, 255, 310, and 355 residues of the Tim50 precursor, respectively, and subjected to *in vitro* transcription/translation reactions as described above. The translation products conjugating with the truncated mRNAs were treated with 2 mM puromycin for 20 min at 30°C to be released from the truncated mRNAs and ribosomes.

To inhibit protein import with specific IgGs, mitochondria (50 μg proteins) and mitoplasts (50 μg proteins) were preincubated with anti-Tim50 IgGs (5-60 μg IgGs) and with IgG prepared from the preimmune serum (30-60 μg IgGs) for 30 min on ice in 180 μl of 250 mM sucrose, 10 mM MOPS-KOH pH 7.4, 10 mM KCl, and 1.33% BSA (for mitochondria) or in 180 μl of 20 mM sucrose, 10 mM MOPS-KOH pH 7.4, 10 mM KCl, and 1.33% BSA (for mitoplasts), and then added 60 μl of 4×Import buffer (250 mM sucrose, 10 mM MOPS-KOH pH 7.4, 290 mM KCl, 8 mM KPi, 8 mM methionine, 20 mM DTT, 20 mM $MgCl_2$, 8 mM ATP, 8 mM NADH) (for mitochondria) or 60 μl of

4×Import buffer without sucrose (for mitoplasts).

2-2-7. Site-specific photocrosslinking with the BPA-containing pb_2(220)-DHFR

Mitochondria were isolated from yeast strain D273-10B (16). The site-specific photocrosslinking with translocation intermediates of radiolabeled pb_2(220)-DHFR containing BPA at residue 94 or residue 114 and the immunoprecipitation of the crosslinked products using anti-Tim50 antibodies and using the preimmune serum were performed according to Kanamori et al. (7). The samples were analyzed by SDS-PAGE and radioimaging with a Storm 860 image analyzer (Amersham Biosciences, Piscataway, NJ, USA).

2-2-8. Chemical crosslinking with pSu9-DHFR accumulated at the TOM channel

Mitochondria were isolated from yeast strains W303-1A and TIM50-3HA (16). Radiolabeled pSu9-DHFR was synthesized as described above, and incubated for 10 min at 30°C with the mitochondria that had been preincubated with 20 μM carbonyl cyanide *m*-chrolophenylhydrazone (CCCP; Sigma-Aldrich, St. Louis, MO, USA) for 5 min on ice to dissipate $\Delta\Psi$. The mitochondria, which contain wild-type Tim50 or Tim50-3HA, were reisolated and subjected to crosslinking with 200 μM *N*-γ-maleimidobutyryloxy-succinimide ester (GMBS; Pierce, Rockford, IL, USA) or 200 mM *m*-maleimidobenzoyl-*N*-hydroxysuccinimide ester (MBS; Pierce, Rockford, IL, USA), respectively, for 60 min on ice in 250 mM sucrose, 10 mM MOPS-KOH pH 7.2, 10 mM KCl, and 10 μM CCCP. After quenching the reaction by addition of 100 mM Tris-HCl pH 7.0, the mitochondria were reisolated and subjected to immunoprecipitation using antibodies against Tim50, Tom40, and Tom22, and using anti-HA monoclonal antibody, according to Kanamori et al. (7). The samples were analyzed by SDS-PAGE and radioimaging with a Storm 860 image analyzer (Amersham Biosciences, Piscataway, NJ, USA).

2-2-9. Preparation of yeast total lysate

The cell pellets of 4 ml of yeast culture (OD_{660} = 0.25) were resuspended in 100 μl of 10 mM Tris-HCl pH 8.0 and 1 mM EDTA, added 6.3 μl of 5 M NaOH and 7 μl of β-mercaptoethanol, and incubated for 4 min on ice. Then, the proteins were precipitated with 10% TCA and boiled in SDS-PAGE sample buffer (125 mM Tris-HCl pH 6.8, 2 mM EDTA, 2% SDS, 100 mg/ml sucrose, 2% β-mercaptoethanol, 30 μg/ml bromophenol blue) for 5 min at 95 ° C. After clarifying centrifugation, the samples were subjected to SDS-PAGE and immunoblotting followed by analyzing with a Storm 860 image analyzer (Amersham Biosciences, Piscataway, NJ, USA).

2-2-10. Measurement of the membrane potential

$\Delta\Psi$ of isolated yeast mitochondria was assessed by using the potential-sensitive fluorescent dye 3,3'-dipropylthiadicarbocyanine iodide ($DiSC_3(5)$; Molecular Probes, Eugene, OR, USA). The fluorescence measurements were performed with a fluorescence spectrophotometer (F-3010; Hitachi, Tokyo, Japan) at 25 ° C, excitation at 622 nm, emission at 670 nm, and slits 5 nm. The following reagents were added to a cuvette and the fluorescence changes were recorded in arbitrary units; 2.2 ml of 600 mM mannitol, 20 mM HEPES-KOH pH 7.4, 40 mM KPi, 0.25% BSA, 5 mM ATP, 15 mM $MgCl_2$, 4.4 μl of 1 mM $DiSC_3(5)$ in DMSO, 25 μl of 10 mg/ml mitochondria, and finally 10 μl of 1 mg/ml valinomycin to dissipate $\Delta\Psi$.

2-2-11. Co-immunoprecipitation and co-purification assay

Co-immunoprecipitation of the complex containing Tim50 was performed as follows. Mitochondria were isolated from yeast strain W303-1A (16). The mitochondria (2 mg/ml proteins) were solubilized with 2% digitonin in co-Lysis buffer (20 mM Tris-HCl pH 7.4, 250 mM NaCl, 1 mM EDTA, 10% glycerol) containing protease inhibitors for 20

min at 4°C, followed by clarifying centrifugation at 20,000 × *g* for 10 min at 4°C. The supernatants were diluted 3-fold with co-Lysis buffer and incubated with Protein A Sepharose 4FF (Amersham Biosciences, Piscataway, NJ, USA) carrying specific antibodies for 6 hr at 4°C with gentle mixing. The resins were washed three times with co-Lysis buffer and boiled in SDS-PAGE sample buffer without β-mercaptoethanol for 5 min at 95°C. The samples were subjected to SDS-PAGE and immunoblotting followed by analyzing with a Storm 860 image analyzer (Amersham Biosciences, Piscataway, NJ, USA).

Co-purification assay of the complex containing Tim50-His6 was performed as follows. Mitochondria were isolated from yeast strains TIM50-HIS6 and TIM50-3HA (16). The mitochondria (1 mg/ml proteins) were solubilized with 1% digitonin in Lysis buffer (50 mM Tris-HCl pH 8.0, 250 mM NaCl) containing 20 mM imidazole and protease inhibitors for 20 min at 4°C, followed by clarifying centrifugation at 20,000 × *g* for 10 min at 4°C. The supernatants were diluted 2-fold with Lysis buffer and incubated with Ni-NTA agarose (Qiagen, Hilden, Germany) for 2 hr at 4°C with gentle mixing. Then, the resins were packed into columns, washed twice with Lysis buffer containing 0.5% digitonin and 20 mM imidazole, and eluted with Lysis buffer containing 0.5% digitonin and 250 mM imidazole. The samples were precipitated with 15% TCA and 0.05% NaDOC, and subjected to SDS-PAGE and immunoblotting followed by analyzing with a Storm 860 image analyzer (Amersham Biosciences, Piscataway, NJ, USA).

2-2-12. Glycerol density gradient centrifugation

Mitochondria were isolated from yeast strain W303-1A (16). The mitochondria (200 μg proteins) were solubilized with 200 μl of 1% digitonin in 20 mM Tris-HCl pH 7.5, 20 mM NaCl, 2 mM EDTA, and 10% glycerol, followed by clarifying centrifugation at 100,000 × *g* for 30 min at 4°C. The supernatant was layered onto 5 ml of 10-40% linear glycerol gradient in 20 mM Tris-HCl pH 7.5, 20 mM NaCl, 2 mM EDTA, and 0.2%

digitonin, and centrifugated at 200,000 × *g* for 15 hr at 4°C. After centrifugation, fractions (275 μl each) were collected from the top and precipitated with 15% TCA and 0.05% NaDOC. The samples were subjected to SDS-PAGE and immunoblotting followed by analyzing with a Storm 860 image analyzer (Amersham Biosciences, Piscataway, NJ, USA).

Table 1. *S. cerevisiae* strains used in this study

Strain	Genotype	Remarks
D273-10B	*MAT*α	
W303-1A	*MAT***a** *ade2-1 his3-11,15 ura3-1 leu2-3,112 trp1-1 can1-100*	
W303-AB	*MAT***a**/α *ade2-1/ade2-1 his3-11,15/his3-11,15 ura3-1/ura3-1 leu2-3,112/leu2-3,112 trp1-1/trp1-1 can1-100/can1-100*	
PJ69-4A	*MAT***a** *trp1-901 leu2-3,112 ura3-52 his3-200 gal4Δ gal80Δ LYS2::GAL1-HIS3 GAL2-ADE2 met2::GAL7-lacZ*	ref. 15
TIM50/tim50::CgHIS3	*MAT***a**/α *ade2-1/ade2-1 his3-11,15/his3-11,15 ura3-1/ura3-1 leu2-3,112/leu2-3,112 trp1-1/trp1-1 can1-100/can1-100 TIM50/tim50::CgHIS3*	this study
GAL7-TIM50	*MAT***a** *ade2-1 his3-11,15 ura3-1 leu2-3,112 trp1-1 can1-100 tim50::CgHIS3-PGAL7-TIM50*	this study
TIM50-3HA	*MAT***a** *ade2-1 his3-11,15 ura3-1 leu2-3,112 trp1-1 can1-100 tim50::CgHIS3* [*CEN6 TRP1 TIM50-3HA*]	this study
TIM50&TIM50-3HA	*MAT***a** *ade2-1 his3-11,15 ura3-1 leu2-3,112 trp1-1 can1-100* [*CEN6 TRP1 TIM50-3HA*]	this study
TIM50-HIS6	*MAT***a** *ade2-1 his3-11,15 ura3-1 leu2-3,112 trp1-1 can1-100 tim50::CgHIS3* [*CEN6 TRP1 TIM50-HIS6*]	this study

2-3. Results

2-3-1. Identification of Tim50 as a crosslinked partner of the translocation intermediate anchored to the inner membrane

Translocation intermediate of pb_2(220)-DHFR containing BPA at position 94 was crosslinked with an unidentified translocator component to generate a 95-kDa crosslinked product (7). In order to identify the crosslinked partner protein, pb_2(220)-DHFR-94C, a pb_2(220)-DHFR derivative that has a unique cysteine residue at position 94 and a hexahistidine tag at the C-terminus was prepared in large amounts from *E. coli* cells (Figure 2-4A). Modification of pb_2(220)-DHFR-94C with a bifunctional chemical crosslinker, NMBz (Figure 2-4B), directs introduction of a photoreactive benzophenone moiety to Cys-94, resulting in the acquisition of the similar structure to the BPA-containing pb_2(220)-DHFR (Figure 2-2).

NMBz-modified or mock-treated pb_2(220)-DHFR-94C was incubated with isolated yeast mitochondria in the presence of MTX to generate translocation intermediates, and then the samples were UV irradiated (Figure 2-5). NMBz-modified pb_2(220)-DHFR-94C, but not mock-treated pb_2(220)-DHFR-94C, yielded a crosslinked product of ~95 kDa by UV irradiation (Figure 2-5, lanes 4, 6, and 8). Since this crosslinked product could be identical to that of the BPA-containing pb_2(220)-DHFR, the mitochondria were solubilized with 6 M urea and the crosslinked product was purified by affinity chromatography for the hexahistidine tag of the fusion protein. The crosslinked product was mainly eluted with 100 mM imidazole (Figure 2-6, left panel, lane 5) and the purity appeared sufficient to identify the crosslinked partner (Figure 2-6, right panel, lane 5). Indeed, the tryptic digestion of the purified crosslinked product followed by mass spectrometry analysis identified four peptides, whose sequences corresponded to the open reading frame (ORF) *YPL063w* on yeast chromosome XVI that encodes a 55,098 Da

polypeptide of an unknown function (Figure 2-7). The predicted product, Ypl063p, consists of 476 amino-acid residues and possesses a predicted N-terminal mitochondrial presequence (residues 1-43) (22) and a putative transmembrane segment (residues 112-132) (Figure 2-8). Indeed, N-terminal peptide sequencing of the 95-kDa crosslinked product showed that the mature part of Ypl063p starts from residue 44 and has a MW of 50,365 Da. According to the established nomenclature for components of the translocator complex (23), I termed this novel protein Tim50. The structural features of Tim50 predict a topology of the integral inner-membrane protein with the N-terminal part (residues 44-111) facing the matrix and the large C-terminal domain (residues 133-476) exposed to the IMS.

Database searches showed that ORFs encoding proteins with similarity to Tim50 and with a putative mitochondrial presequence are found in the genomes of evolutionarily distant organisms, including *Candida albicans* (orf6.6573 [43.3% identical residues/ 79.7% similarity]), *Schizosaccharomyces pombe* (SPBC8D2.21C [34.1%/67.5%]), *Neurospora crassa* (AAO32939 [27.8%/50.0%]), *Caenorhabditis elegans* (T21C9.12 [23.5%/53.1%]), *Drosophila melanogaster* (CG12313 [21.0%/51.8%]), *Mus musculus* (NP_079892 [26.1%/58.1%]), and *Homo sapiens* (XP_053074 [19.7%/45.2%]) (Figure 2-9). These Tim50 homologs in the other organisms have a possible transmembrane segment near the N-terminus, so that they likely take the same N_{in}-C_{out} topology in the inner membrane as yeast Tim50. *S. cerevisiae* also has three other proteins that are homologous to Tim50 and function as CTD-like phosphatases (24), but exhibit different localizations, namely Nem1p in the nuclear/ER membrane (25) and Psr1p and Psr2p in the plasma membrane (26). However, the active site residues of the D*X*D*X*(T/V) motif (24, 27), which is essential for their phosphatase activity, are not conserved in Tim50.

To confirm that the crosslinked products arising from the MTX-arrested translocation intermediates of pb_2(220)-DHFR containing BPA at positions 94 or 114 possess Tim50, I raised the specific antibodies against the C-terminal segment (residues

242-476) of Tim50 (Figure 2-10A). The resultant antibodies recognized both 50-kDa and 54-kDa proteins for mitochondria containing both wild-type Tim50 (50,365 Da) and C-terminally 3HA-tagged Tim50 (Tim50-3HA) (53,618 Da), or only 54-kDa protein for mitochondria containing Tim50-3HA instead of wild-type Tim50 (Figure 2-10B), indicating that the resultant antibodies could recognize the Tim50 epitopes. After formation of the MTX-arrested translocation intermediates of pb_2(220)-DHFR containing BPA at positions 94 or 114 as described previously (7), UV irradiation yielded the ~95-kDa or ~102-kDa crosslinked products, respectively (Figure 2-11). The crosslinked products were specifically immunoprecipitated with the antibodies against Tim50, but not with the preimmune serum (Figure 2-11). These results indicate that the crosslinked partner responsible for the 95-kDa crosslinked product is indeed Tim50.

2-3-2. Tim50 is an essential inner-membrane protein of yeast mitochondria

To assess the functions of Tim50, the *TIM50* gene was disrupted in the diploid yeast strain by integration of the *HIS3* gene of *Candida glabrata* (*CgHIS3*), the cells were induced to sporulate, and the four spores were subjected to tetrad analysis. Upon dissection, each tetrad yielded only two viable spores (Figure 2-12A). All viable spores showed his^- selectivities and were confirmed to carry the non-disrupted *TIM50*. When transformed with the *CEN6-TRP1* plasmid carrying the *TIM50* gene, but not with the vector alone, the *TIM50*-disrupted diploid cells yielded three or four viable spores after tetrad analysis (Figure 2-12B). One or two spores out of the three or four viable spores, respectively, showed his^+trp^+ selectivities and were confirmed to carry the *CgHIS3* marker instead of the *TIM50* gene and to suppress their lethality with the plasmid-derived *TIM50* gene. These results indicate that *TIM50* is an essential gene for yeast cell viability.

Since Tim50 carries a putative mitochondrial targeting presequence, I analyzed its subcellular location by indirect immunofluorescence microscopy. Staining of yeast cells

with the anti-Tim50 antibodies showed a tubular network in the cytoplasm (Figure 2-13, left). This staining is typical for yeast mitochondrial proteins, and nearly identical staining was observed with the antibody against mitochondrial porin (Figure 2-13, center). Thus, Tim50 is a mitochondrial protein.

Then, I isolated yeast mitochondria and analyzed the submitochondrial location of Tim50. Tim50 was inaccessible to protease added to intact mitochondria (Figure 2-14, lanes 1 and 2), but was accessible to protease added to mitoplasts, where the outer membrane was selectively ruptured (Figure 2-14, lanes 3 and 4). This behavior resembles that of Tim23, an inner-membrane protein exposing a domain to the IMS, but is different from those of Tom70, an outer-membrane protein exposing a domain to the cytosol, or subunit β of F_1-ATPase ($F_1\beta$), a peripheral inner-membrane protein on the matrix side (Figure 2-14). Tim50 was, like integral membrane proteins, Tom70 and Tim23, not extracted from the membranes with Na_2CO_3 at pH 11.5 while a peripheral membrane protein, $F_1\beta$, was extracted with Na_2CO_3 (Figure 2-14, lanes 5 and 6). All these proteins were extracted from the membranes with Triton X-100 (Figure 2-14, lanes 7 and 8). These results indicate that Tim50 is an integral membrane protein of the mitochondrial inner membrane. Tim50 became unrecognizable by the antibodies against the C-terminal segment of Tim50 after protease treatments of the mitoplasts. Since Tim50 has only a single putative transmembrane segment near the N-terminus, Tim50 most likely takes the N_{in}-C_{out} topology in the inner membrane and exposes the large C-terminal domain (residues 133-476) to the IMS.

To further confirm that Tim50 is the inner-membrane protein of mitochondria, radiolabeled Tim50 precursor was synthesized in rabbit reticulocyte lysates and incubated with isolated mitochondria in the presence or absence of $\Delta\Psi$ or in the presence or absence of chelating reagents. Since MPP requires Mn^{2+} for its processing-peptidase activity, the chelating reagents are able to inhibit the MPP functions. The Tim50 precursor was

converted to the mature form in the presence of $\Delta\Psi$ (Figure 2-15A, lane 1), but was not in the absence of $\Delta\Psi$ (Figure 2-15A, lane 2) or in the presence of chelating reagents (Figure 2-15A, lane 3). These results indicate that import of the Tim50 precursor strictly requires $\Delta\Psi$ and the Tim50 precursor likely receives the cleavage of the presequence by MPP. When incubated with isolated mitochondria in the presence of $\Delta\Psi$, Tim50 precursor was efficiently converted to the mature form as described above, but was only slowly sequestered to the inner compartment that was protected from protease added to the mitochondria (Figure 2-15B, Figure 2-16). These results indicate that the N-terminus of Tim50 can reach the matrix efficiently while the C-terminal domain of Tim50 traverses across the outer membrane slowly *in vitro*.

The slow rate of the *in vitro* import of Tim50 precursor into mitochondria might be due to the folded structure of the C-terminal domain of the Tim50 precursor, which is resistant to moderate protease digestion resulting in the generation of ~28-kDa fragment of Tim50 precursor (Figure 2-17). Indeed, C-terminally truncated versions of the Tim50 precursor, which consist of the residues 1-225, residues 1-255, residues 1-310, or residues 1-355 of the Tim50 precursor, were efficiently imported into mitochondria, in contrast to the full-length Tim50 precursor (Figure 2-18). *In vivo*, Tim50 is likely imported into mitochondria in a co-translational manner because it is synthesized on membrane-bound polysomes (28).

2-3-3. Tim50 mediates translocation of presequence-containing precursor proteins across the inner membrane

Since Tim50 is crosslinked to the translocation intermediate of pb_2(220)-DHFR, Tim50 may mediate import of precursor proteins into mitochondria. I constructed a yeast strain GAL-TIM50, in which the galactose-inducible *GAL7* promoter was integrated into the chromosome in front of the *TIM50* gene, allowing regulated expression of Tim50.

Since Tim50 is essential for yeast cell viability, GAL-TIM50 cells grew on galactose-containing medium (YPGal), but not on glucose-containing medium (YPD) (Figure 2-19A). Total lysates were prepared from yeast wild-type cells or from GAL-TIM50 cells, various times after the shift from YPGal to YPD, and were analyzed by immunoblotting for various mitochondrial proteins (Figure 2-19B). When cultivated in the presence of galactose, the level of Tim50 in GAL-TIM50 cells was 2.5-fold higher than in wild-type cells (Figure 2-19B, lane 3, Tim50). However, the levels of Tim50 decrease with the time of cultivation in YPD and reach 7.5% of that in wild-type cells 24 hr after the shift to YPD (Figure 2-19B, lane 6, Tim50). Depletion of Tim50 did not severely affect the expression levels of other proteins involved in the mitochondrial protein import, such as Tom40, Tom22, Tim23, Tim17, Tim44, and Ssc1p (Figure 2-19B). On the other hand, prolonged cultivation of GAL-TIM50 cells in the absence of galactose led to accumulation of uncleaved precursor forms of mitochondrial heat shock protein Hsp60 (mtHsp60) and Mdj1p (Figure. 2-19B, mtHsp60 and Mdj1p). The level of phosphate carrier (PiC), a presequence-less polytopic inner-membrane protein, was not significantly affected by depletion of Tim50 as compared with the wild-type strain. Therefore, reduction of the level of Tim50 apparently caused defects in import of presequence-containing mitochondrial proteins *in vivo*.

In parallel, the effects of depletion of Tim50 were tested on mitochondrial protein import *in vitro*. First, mitochondria were isolated from wild-type cells or GAL-TIM50 cells (Tim50↓ cells) after cultivation in galactose-free medium for 12 hr. The amounts of Tim50 in Tim50↓ mitochondria was 19% of that of WT mitochondria and the $\Delta\Psi$ of Tim50↓ mitochondria was virtually identical to that of WT mitochondria (Figure 2-20). Then, import of the radiolabeled presequence-containing precursor of mtHsp60 and radiolabeled pSu9-DHFR, a fusion protein between the presequence of subunit 9 of F_o-ATPase and DHFR, into WT mitochondria and into Tim50↓ mitochondria was monitored. The rates of import of the mtHsp60 precursor and pSu9-DHFR into Tim50↓ mitochondria were

significantly decreased as compared with those into wild-type mitochondria (Figure 2-21A and 2-21B). I observed similar decrease in import rates of pb_2(220)-DHFR into Tim50↓ mitochondria (Figure 2-21C). Moreover, import of ADP/ATP carrier (AAC), a presequence-less polytopic inner-membrane protein, into Tim50↓ mitochondria was compared with that into wild-type mitochondria. In contrast to mtHsp60 precursor, pSu9-DHFR, and pb_2(220)-DHFR, neither translocation across the outer membrane nor insertion into the inner membrane for AAC was affected by depletion of Tim50 (Figure 2-21D and 2-21E).

To confirm that Tim50 is directly involved in mitochondrial protein import, I tested the effects of antibodies against Tim50 on protein import into mitochondria and into mitoplasts *in vitro*. Anti-Tim50 antibodies inhibit the Tim50 functions when incubated with mitoplasts to reach the IMS-exposed region of Tim50. Mitochondria and mitoplasts were preincubated with immunoglobulins G (IgGs) prepared from the anti-Tim50 antiserum and from the preimmune serum, and subsequently incubated with radiolabeled mtHsp60 precursor, pSu9-DHFR, and Tim23. Like AAC, Tim23 is imported into mitochondria via the TOM complex and inserted into the inner membrane with the aid of the TIM22 complex instead of the TIM23 complex. While import of mtHsp60 precursor and pSu9-DHFR into mitochondria was not affected by preincubation with anti-Tim50 IgGs, the import rates of mtHsp60 precursor and pSu9-DHFR into mitoplasts were significantly decreased by preincubation with anti-Tim50 IgGs, but not with the control IgGs (Figure 2-22). The amounts of anti-Tim50 IgG required for inhibition of the import of mtHsp60 precursor and pSu9-DHFR into mitoplasts were < 5 μg IgGs per 50 μg mitochondrial proteins (Figure 2-23). On the other hand, insertion of Tim23 into the inner membrane was not affected by preincubation of mitochondria or mitoplasts with anti-Tim50 IgGs (Figure 2-23). These results indicate that Tim50 mediates the early step of translocation of mitochondrial precursor proteins with a cleavable presequence, but not the ones without a presequence,

across the inner membrane.

2-3-4. Tim50 is a subunit of the TIM23 complex

Since Tim50 is directly involved in the translocation of presequence-containing precursor proteins, but not of presequence-less preproteins, across the inner membrane, Tim50 can be a component of the TIM23 complex, a translocator for presequence-containing precursor proteins. I thus asked if Tim50 is associated with the subunits of the TIM23 complex in mitochondria. Mitochondria were solubilized with 2% digitonin and subjected to immunoprecipitation with antibodies against Tim50, Tim23, and Tom40. The immunoprecipitates were then analyzed for Tim50 and Tim23, the main component of the TIM23 complex, by SDS-PAGE and immunoblotting. Tim50 was co-immunoprecipitated with anti-Tim23 antibodies, but not with anti-Tom40 antibodies. Conversely, anti-Tim50 antibodies immunoprecipitated Tim23 together with Tim50 (Figure 2-24A).

To obtain additional evidence that Tim50 is a subunit of the TIM23 complex, mitochondria containing C-terminally hexahistidine-tagged Tim50 (Tim50-His6) were solubilized and subjected to incubation with Ni-NTA agarose. Tim50-His6 efficiently bound to Ni-NTA agarose and was eluted with 250 mM imidazole (Figure 2-24B, lanes 4-6). The subunits of the TIM23 complex, Tim23, Tim17, and Tim44 were also adsorbed to Ni-NTA agarose and were eluted with 250 mM imidazole, while Tom70 or AAC did not bind to the resin (Figure 2-24B, lanes 4-6). As a control, when solubilized mitochondria containing Tim50-3HA instead of Tim50-His6 were incubated with Ni-NTA agarose, neither Tim50 nor other subunits of the TIM23 complex bound to the resin (Figure 2-24B, lanes 1-3). These results indicate that Tim50 is a subunit of the TIM23 complex.

To assess the molar ratio of Tim50 in the TIM23 complex, mitochondria were solubilized with 1% digitonin and analyzed by glycerol density gradient centrifugation. Tim50 was recovered partly in the fractions corresponding to ~140 kDa and partly in those

corresponding to ~250 kDa (Figure 2-25). Since Tim23 was recovered in the fractions corresponding to ~250 kDa (Figure 2-25), about one third of the Tim50 molecules are apparently associated with the TIM23 complex. By standardized immunoblotting in comparison with the purified Tim50 fragment expressed in *E. coli* cells, yeast mitochondria were found to contain ~30 pmol of Tim50 per mg of mitochondrial proteins (Figure 2-26), while they were reported to contain approximately 17-20 pmol of Tim23 per mg of mitochondrial proteins (29, 30). Therefore, the molar ratio of Tim50:Tim23 in the TIM23 complex is roughly estimated to be 1:2 in this experimental condition.

To further analyze the interactions between Tim50 and Tim23, I used a yeast two-hybrid analysis. To this end, a fusion gene for the activator domain of yeast Gal4p and the IMS domain (residues 133-476) of Tim50 and those for the DNA binding domain of yeast Gal4p and three segments (residues 1-50, residues 51-96, and residues 1-96) of the N-terminal half of Tim23 was constructed. After confirming the expression of the corresponding fusion proteins in yeast cells, it was asked which combinations of the fusion genes expressed together with a reporter gene, *GAL2-ADE2*, in yeast cells give rise to ade$^+$ colonies. Interactions between the two fusion proteins will lead to the localization of Gal4p to the DNA, thereby activating the *GAL2*-regulated allele of *ADE2* (15). The IMS domain of Tim50 fused to the Gal4p activator domain gave rise to ade$^+$ colonies when Tim23(51-96) or Tim23(1-96), but not Tim23(1-50), fused to the Gal4p DNA binding domain was co-expressed (Figure 2-27A). This suggests that the IMS domain of Tim50 directly interacts with residues 51-96 of Tim23. It has been reported that Tim23 takes an unusual transmembrane topology in which Tim23 spans both the outer and inner membranes (31); the N-terminal domain (residues 1-50) is integrated into the outer membrane and exposes the extreme N-terminus to the cytosol, while the C-terminal half (residues 100-222) is integrated into the inner membrane, leaving residues 50-100 between the two domains exposed to the IMS. Therefore, the results of the yeast two-hybrid

analysis show that the IMS domain of Tim50 can interact with the possible IMS-exposed segment of Tim23 (Figure 2-27B).

I next tested if protease accessibility of the N-terminus of Tim23 is affected by overexpression or depletion of Tim50 in mitochondria. About half of the Tim23 molecules in wild-type mitochondria were clipped and a resistant fragment Tim23* was generated when intact mitochondria were treated with proteinase K (Figure 2-28), as reported previously (31). The fraction of Tim23* that received the N-terminal cleavage decreased in mitochondria with decreased Tim50 (Tim50↓), whereas it increased in mitochondria with overexpressed Tim50 (Tim50↑). These results suggest that the integration of the N-terminal segment of Tim23 into the outer membrane is dynamic and is stabilized by Tim50. Since Tim50 excess over the wild-type level of Tim50 still affects the clipping of Tim23, interactions of Tim50 with the TIM23 complex may be also dynamic.

2-3-5. Tim50 links protein translocation across the outer and inner membranes

The N-terminal domain (residues 1-50) of Tim23 has been suggested to facilitate the transfer of precursor proteins from the TOM complex to the TIM23 complex (31). Since Tim50 has a large C-terminal domain exposed to the IMS, which interacts with the IMS-exposed segment of Tim23, Tim50 may also facilitate the transfer of precursor proteins between the TOM and TIM23 complexes. To test such a possibility, the interactions of the translocation intermediate accumulated at the TOM complex with Tim50 was probed by a crosslinking approach.

pSu9-DHFR binds to the mitochondrial surface when incubated with isolated mitochondria containing wild-type Tim50 or Tim50-3HA that have been treated with CCCP to prevent the presequence translocation across the inner membrane by dissipating $\Delta\Psi$ (32). In this intermediate, the presequence of pSu9-DHFR reaches the *trans* site of the TOM complex and the DHFR domain is unfolded and bound to Tom40 (32). Then the

mitochondria were reisolated and treated with hetero-bifunctional crosslinker, MBS or GMBS, for amino groups and sulfhydryl groups. The crosslinked partners were identified by solubilization of the mitochondria followed by immunoprecipitation with specific antibodies against the known components of the TOM and TIM23 complexes.

Figure 2-29 shows the crosslinked products and their assignments to components of the TOM and TIM23 complexes. The crosslinking partners for ~92-kDa and ~60-kDa crosslinked products were assigned to Tom40, and that for ~45-kDa crosslinked products to Tom22. pSu9-DHFR contains a cysteine residue at position 76 (residue 7 in the DHFR domain) and Tom40 at positions 165, 326, 341, and 355, but Tom22 does not have a cysteine residue. Therefore, while there are many possibilities for the cysteine residues involved in the crosslinking between pSu9-DHFR and Tom40, Tom22 should be crosslinked to a single cysteine residue near the N-terminus of the DHFR domain of pSu9-DHFR.

Anti-Tim50 antibodies immunoprecipitated ~75-kDa and ~65-kDa crosslinked products for mitochondria containing wild-type Tim50 and a ~90-kDa crosslinked product for those containing Tim50-3HA (Figure 2-29). Although the band of the ~90-kDa crosslinked product for the mitochondria containing Tim50-3HA was partly overlapped by that of the crosslinked product involving Tom40, the ~90-kDa product was immunoprecipitated with the anti-HA antibody, but not with anti-Tom22 antibodies. A single cysteine residue at position 268 of Tim50 is likely crosslinked to the presequence of pSu9-DHFR, which contains several amino groups. Therefore, the translocation intermediate lodged in the TOM channel is already interacting with Tim50 of the TIM23 complex, suggesting the role of Tim50 in linking translocation mediated by the TOM complex and that mediated by the TIM23 complex.

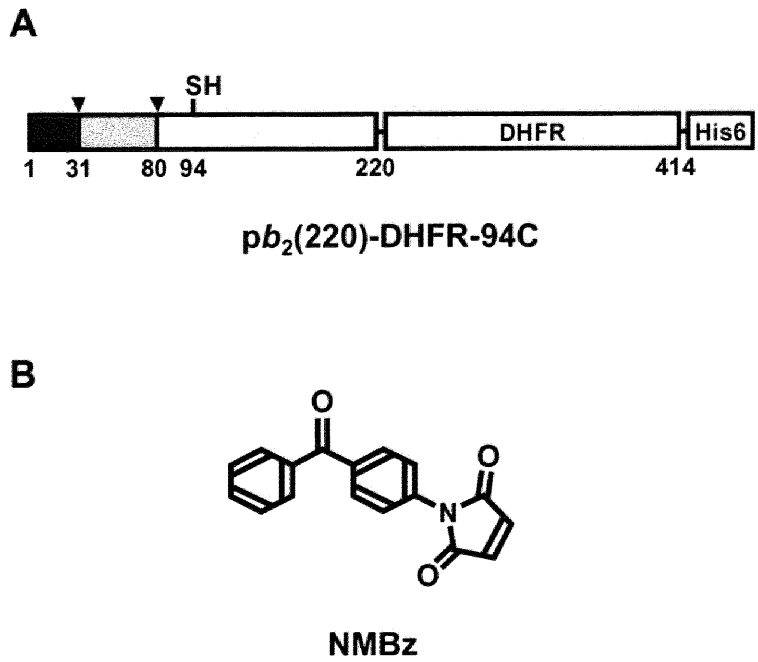

Figure 2-4. Schematic representation of the fusion protein pb_2(220)-DHFR-94C and chemical structure of the photoreactive crosslinker NMBz

(A) The fusion protein pb_2(220)-DHFR-94C is a pb_2(220)-DHFR derivative (see Figure 2-2A) that has a unique cysteine residue at position 94 and a hexahistidine tag at the C-terminus. Modification of pb_2(220)-DHFR-94C with NMBz directs introduction of a photoreactive benzophenone moiety to Cys-94. SH, sulfhydryl group of Cys-94 ;His6, hexahistidine tag.

(B) Chemical structure of the photoreactive crosslinker NMBz. NMBz, 4-(*N*-maleimido)benzophenone.

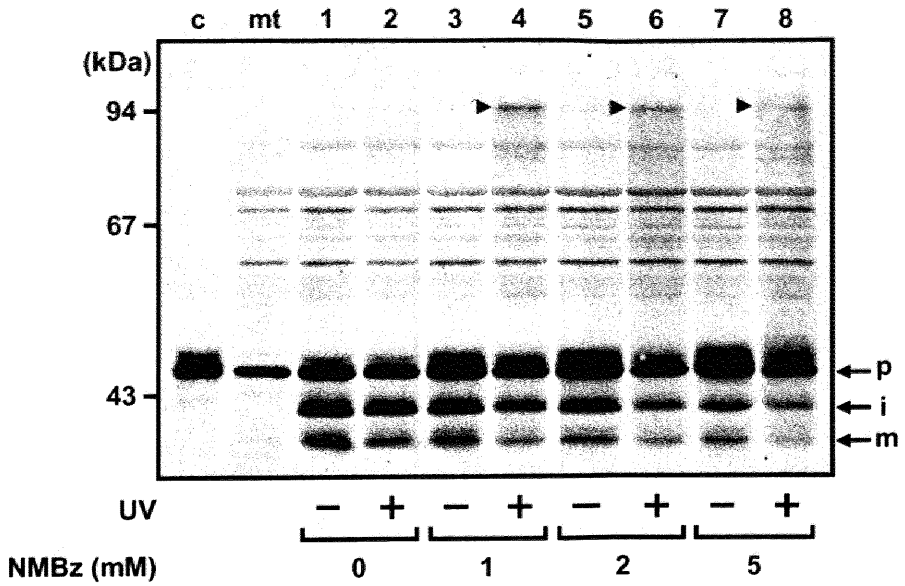

Figure 2-5. NMBz-modified pb_2(220)-DHFR-94C yields the 95-kDa crosslinked product

pb_2(220)-DHFR-94C was preincubated with 0-5 mM NMBz, and then incubated with isolated yeast mitochondria in the presence of MTX to form a translocation intermediate. The samples were divided into halves, and one aliquot was kept on ice (lanes 1, 3, 5, and 7) and the other was UV irradiated (lanes 2, 4, 6, and 8). The mitochondria were reisolated and proteins were analyzed by SDS-PAGE and immunoblotting with anti-DHFR antibodies. Arrowheads indicate the 95-kDa crosslinked products. c, 10% of pb_2(220)-DHFR-94C added to each sample; mt, mitochondria; NMBz, modification with NMBz; UV, UV irradiation; p, i, and m, precursor, processing-intermediate, and mature forms of pb_2(220)-DHFR-94C, respectively.

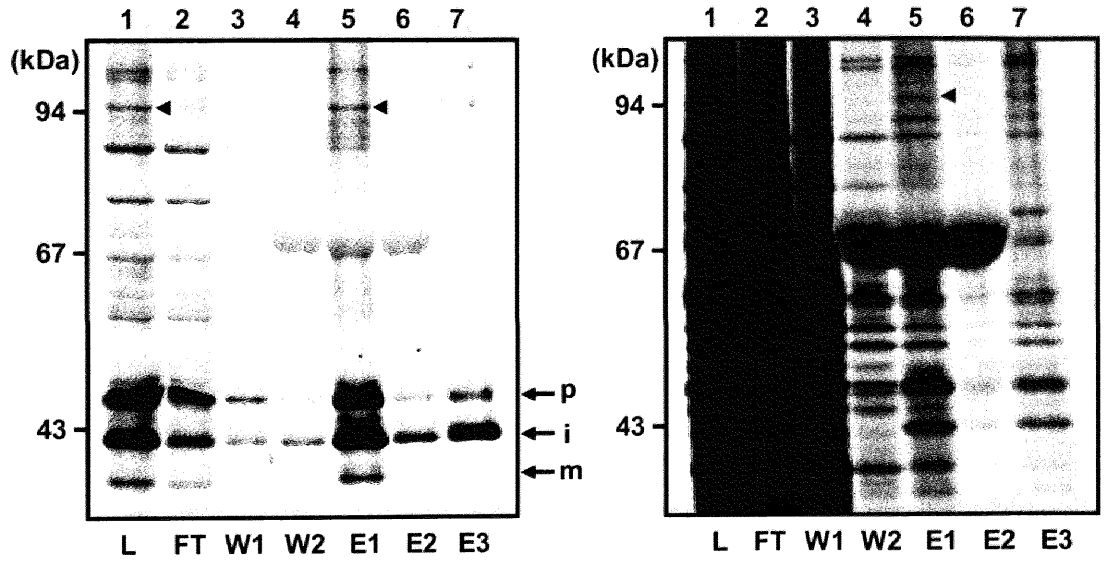

Figure 2-6. Purification of the 95-kDa crosslinked product

After photocrosslinking reaction, the mitochondria were reisolated, solubilized with 6 M urea, and incubated with His-Bind resin, which was subsequently washed twice with 20 mM imidazole. The proteins bound to the resin were eluted twice with 100 mM imidazole and once with 100 mM EDTA. The proteins were analyzed by SDS-PAGE and immunoblotting with anti-DHFR antibodies (left panel) or silver staining (right panel). Arrowheads indicate the 95-kDa crosslinked products. L, loaded sample; FT, flow-through fraction; W1 and W2, washed fractions with 20 mM imidazole; E1 and E2, eluted fractions with 100 mM imidazole; E3, eluted fraction with 100 mM EDTA; p, i, and m, precursor, processing-intermediate, and mature forms of pb_2(220)-DHFR-94C, respectively.

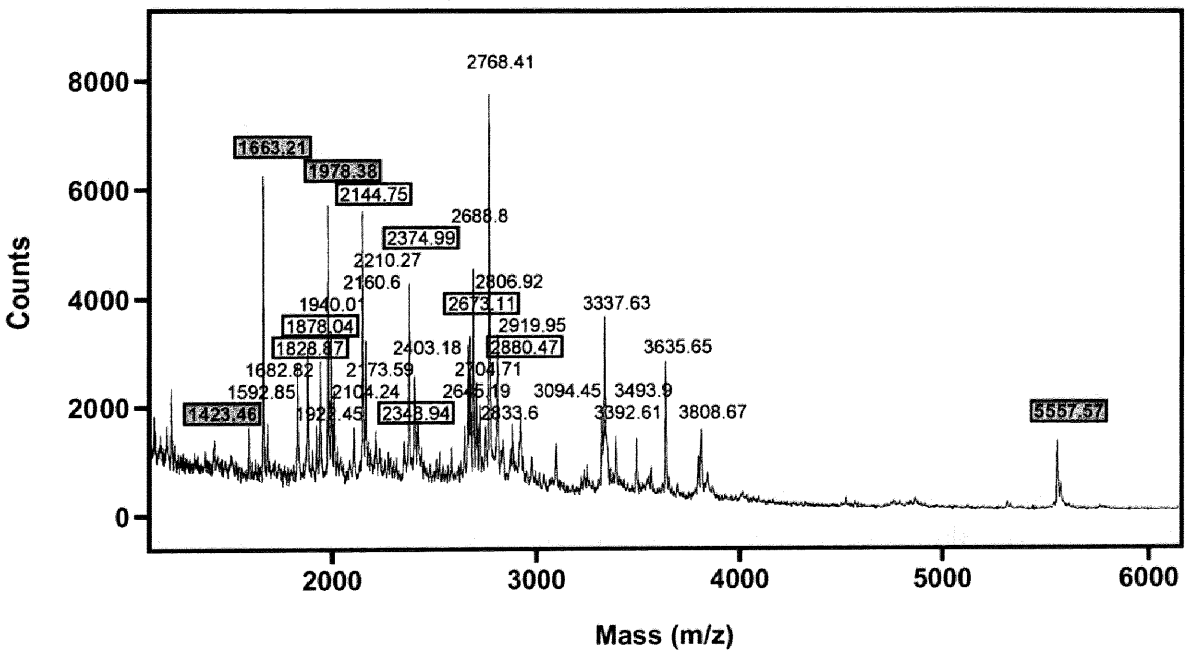

Figure 2-7. Mass spectrum of the tryptic-digestion mixture of the 95-kDa crosslinked product

The purified crosslinked product was subjected to tryptic digestion followed by mass spectrometry analysis and database search. The digested fragments derived from the translation product of the open reading frame *YPL063w* (*TIM50*) are shown in gray and those from pb_2(220)-DHFR-94C in white.

A

MLSILRNSVR LNSRALRVVP SAANTLTSVQ ASRRLLTSYS SFLQKETKDD
KPKSILTDDM LFKAGVDVDE KGQGKNEETS GEGGEDKNEP SSKSEKSRRK
RQTSTDIKRE KVANWFYIFS LSALTGTAIY MARDWEPQES EELKKDIDNG
YTLSLMYKRF KARFNSMFTY FQEPPFPDLL PPPPPPPYQR PLTLVITLED
FLVHSEWSQK HGWRTAKRPG ADYFLGYLSQ YYEIVLFSSN YMMYSDKIAE
KLDPIHAFVS YNLFKEHCVY KDGVHIKDLS KLNRDLSKVI IIDTDPNSYK
LQPENAIPME PWNGEADDKL VRLIPFLEYL ATQQTKDVRP ILNSFEDKKN
LAEEFDHRVK KLKDKFYGDH KSGGNWAMTA LGLGNSLGGS TKFPLDLIHE
EGQKNYLMFM KMIEEEKEKI RIQQEQMGGQ TFTLKDYVEG NLPSPEEQMK
IQLEKQKEVD ALFEEEKKKK KIAESK

B

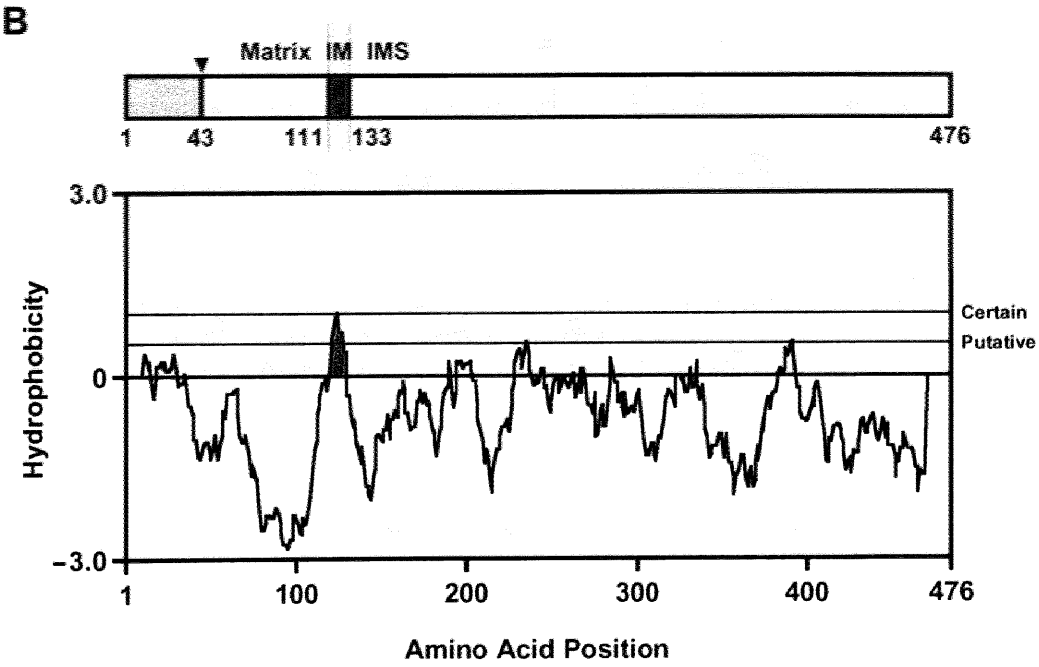

Figure 2-8. Amino-acid sequence and hydropathy profile of Tim50

(A) Deduced amino-acid sequence of Tim50. Tim50 consists of 476 amino-acid residues (MW; 55,098 Da) and possesses a putative mitochondrial presequence (residues 1-43; shown in white), which is cleaved off by MPP, and a potential transmembrane segment (residues 112-132; shown in gray). The predicted mature form of Tim50 consists of 433 amino-acid residues (MW; 50,365 Da). Four peptides identified by tryptic digestion of the crosslinked product followed by mass spectrometry analysis are underlined.
(B) Hydropathy profile of Tim50 was analyzed by the algorism of Kyte-Doolittle (33). Tim50 likely takes an N_{in}-C_{out} topology with the N-terminal part (residues 44-111) in the matrix and the large C-terminal domain (residues 133-476) in the IMS. Vertical arrowhead indicates the putative processing site by MPP. IMS, intermembrane space; IM inner membrane.

Figure 2-9. Multiple sequence alignment of Tim50 homologs

Tim50 homologs of various organisms were aligned by the Clustal W program (34). Asterisks indicate identical amino-acid residues. ":" and "." indicate conserved and semi-conserved substitutions, respectively. Small or hydrophobic residues (A, V, F, P, M, I, L, and W) are shown in brown, acidic residues (D and E) in blue, basic residues (R and K) in red, and other residues (S, T, Y, H, C, N, G, and Q) in green. The potential transmembrane segments are boxed. Sc, *S. cerevisiae*; Ca, *C. albicans*; Sp, *S. pombe*; Nc, *N. crassa*; Ce, *C. elegans*; Dm, *D. melanogaster*; Mm, *M. musculus*; Hs, *H. sapiens*.

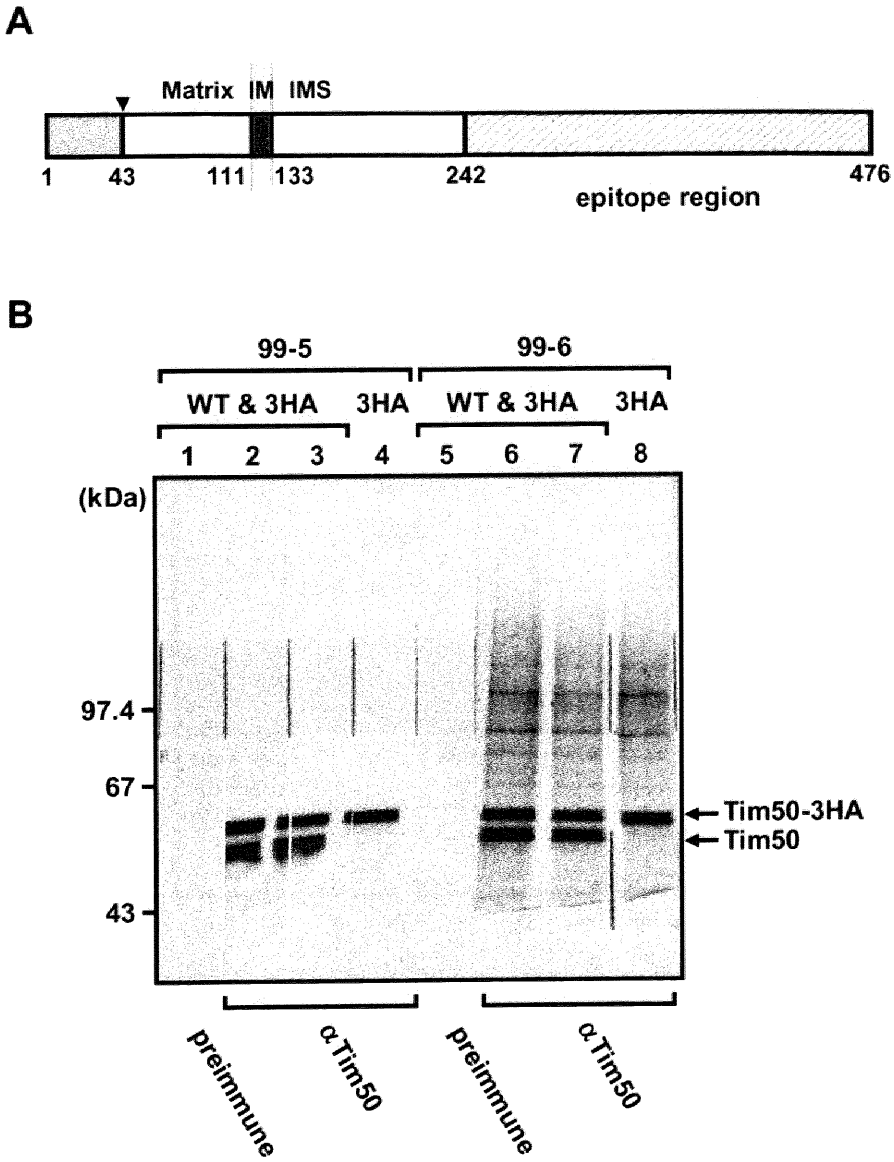

Figure 2-10. Construction of specific antibodies against Tim50

(A) The epitope region of anti-Tim50 antibodies constructed in this study is schematically shown. The C-terminal segment of Tim50 (residues 242-476) was purified from *E. coli* cells and used for immunizing rabbits for obtaining specific antibodies against Tim50.
(B) Mitochondria were prepared from yeast strain expressing both wild-type Tim50 and Tim50-3HA (WT & 3HA) and yeast strain expressing Tim50-3HA instead of wild-type Tim50 (3HA). The mitochondria were subjected to SDS-PAGE and immunoblotting with anti-Tim50 antibodies (αTim50) and the preimmune serum (preimmune). 99-5 and 99-6 indicate the arbitrary numbers of rabbits.

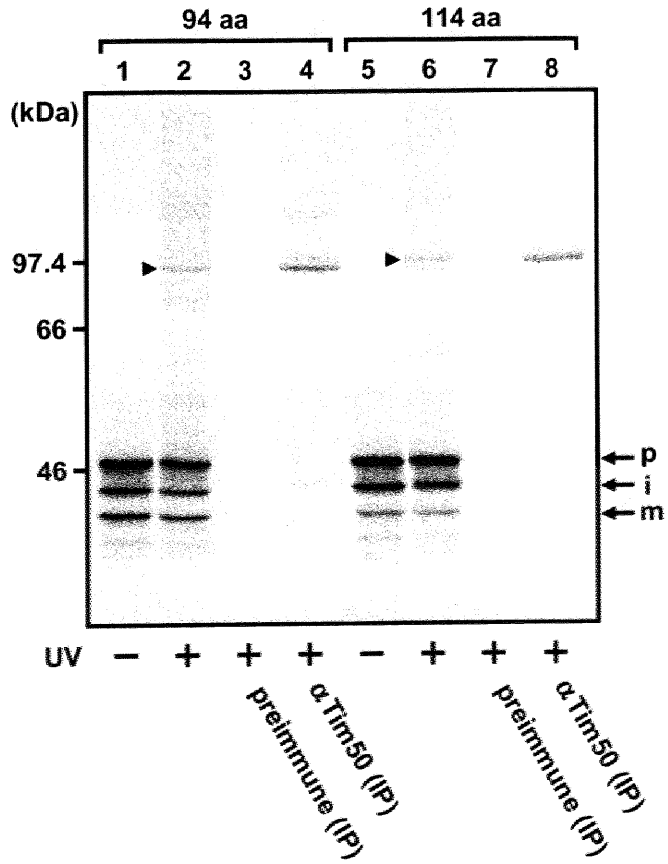

Figure 2-11. Translocation intermediates of pb_2(220)-DHFR containing BPA at residues 94 or 114 are crosslinked with Tim50

Radiolabeled pb_2(220)-DHFR containing BPA at residue 94 (94 aa) or residue 114 (114 aa) were incubated with mitochondria for 20 min at 30°C in the presence of MTX, and then UV irradiated (lanes 2-4 and 6-8). Crosslinked products were analyzed by immunoprecipitation with anti-Tim50 antibodies (αTim50 (IP)) and the preimmune serum (preimmune (IP)). The immunoprecipitates were analyzed by SDS-PAGE and radioimaging. Arrowheads indicate the crosslinked products. UV, UV irradiation; p, i, and m, precursor, processing-intermediate, and mature forms of pb_2(220)-DHFR, respectively.

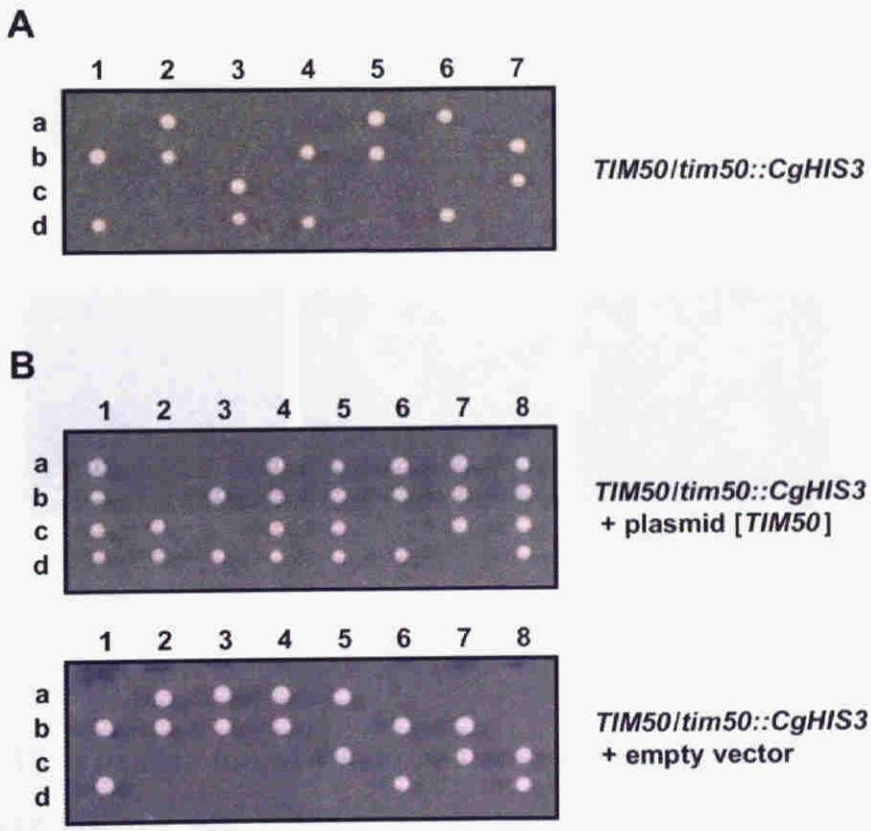

Figure 2-12. Tim50 is essential for yeast cell viability

(A) One of the two chromosomal *TIM50* genes in yeast diploid strain W303-AB was disrupted by integration of the *C. glabrata HIS3* gene, the diploid cells were sporulated, and seven different asci were dissected. The four spores recovered from each of the asci were allowed to germinate and to grow on YPD for 3 days at 30°C.

(B) *TIM50*-disrupted diploid strain was transformed with the *TIM50*-containing plasmid (upper panel) or with the empty vector (lower panel), and subjected to sporulation followed by tetrad analysis as described in (A).

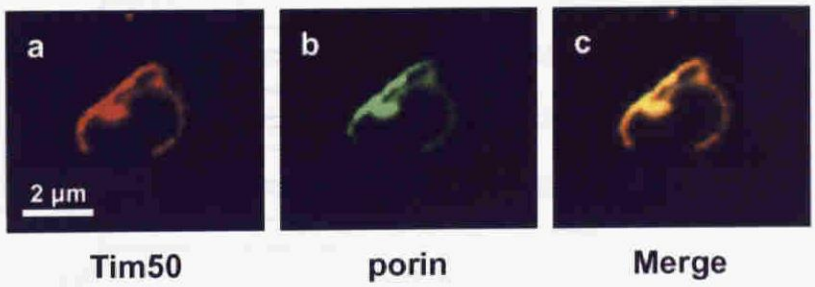

Figure 2-13. Localization of Tim50 by immunofluorescence microscopy

Cells of yeast wild-type strain W303-1A were analyzed by double-label immunofluorescence microscopy using anti-Tim50 antibodies and anti-porin monoclonal antibody. Panels *a*, *b*, and *c* show the same field of the fluorescent images stained with anti-Tim50 antibodies (red) or anti-porin antibodies (green), and of the merged image, respectively.

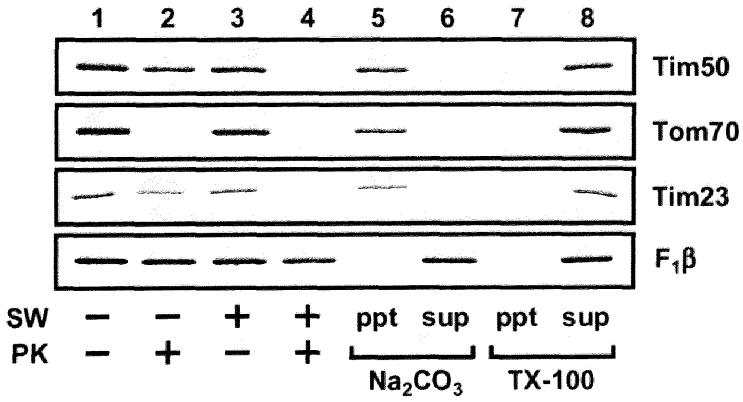

Figure 2-14. Submitochondrial localization of Tim50

Mitochondria were converted to mitoplasts by osmotic swelling (lanes 3 and 4) and treated with 200 μg/ml proteinase K for 20 min on ice (lanes 2 and 4). Mitochondria were treated with either 0.1 M Na_2CO_3 (lanes 5 and 6) or 1% Triton X-100 (lanes 7 and 8), and then pellets (ppt) and supernatants (sup) were separated by centrifugation. The samples were analyzed by SDS-PAGE and immunoblotting with antibodies against Tim50, Tom70, Tim23, and $F_1\beta$. SW, osmotic swelling; PK, proteinase K treatment; Na_2CO_3, extraction with Na_2CO_3; TX-100, extraction with Triton X-100; ppt, pellet fraction; sup, supernatant fraction.

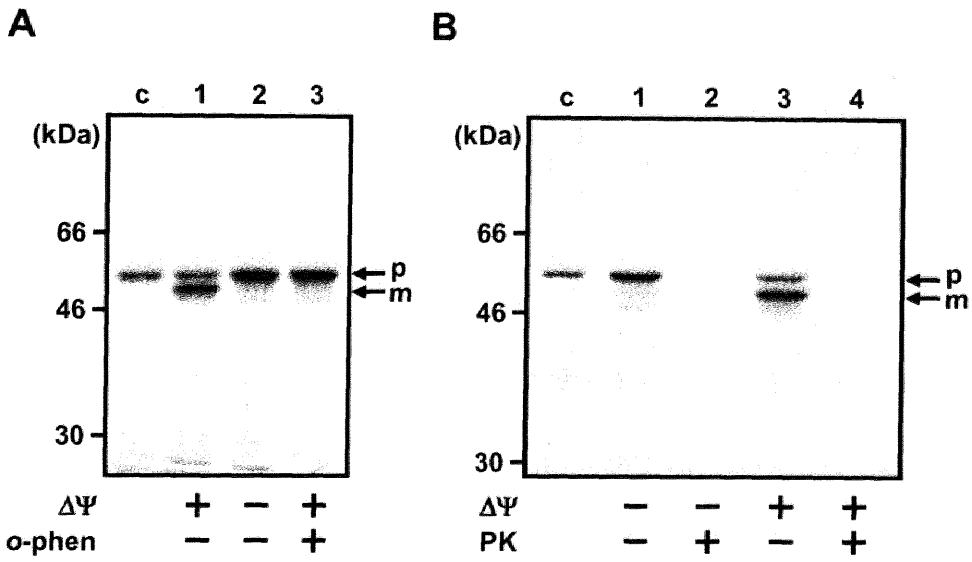

Figure 2-15. *In vitro* import of Tim50 precursor into isolated mitochondria

(A) Radiolabeled Tim50 precursor was incubated with isolated mitochondria for 20 min at 30°C in the presence (lanes 1 and 3) or absence (lane 2) of ΔΨ, or in the presence (lane 3) or absence (lanes 1 and 2) of *o*-phenanthroline and EDTA. The mitochondria were reisolated and proteins were analyzed by SDS-PAGE and radioimaging. c, 25% of the Tim50 precursor added to each sample; ΔΨ, membrane potential; *o*-phen, addition of *o*-phenanthroline and EDTA; p and m, precursor and mature forms of Tim50, respectively.
(B) Radiolabeled Tim50 precursor was incubated with isolated mitochondria for 20 min at 30°C in the presence (lanes 3 and 4) or absence (lanes 1 and 2) of ΔΨ. The samples were divided into halves, and one aliquot was kept on ice (lanes 1 and 3) and the other was treated with 100 μg/mg proteinase K for 20 min on ice (lanes 2 and 4). The mitochondria were reisolated and proteins were analyzed by SDS-PAGE and radioimaging. c, 25% of the Tim50 precursor added to each sample; ΔΨ, membrane potential; PK, proteinase K treatment, p and m, precursor and mature forms of Tim50, respectively.

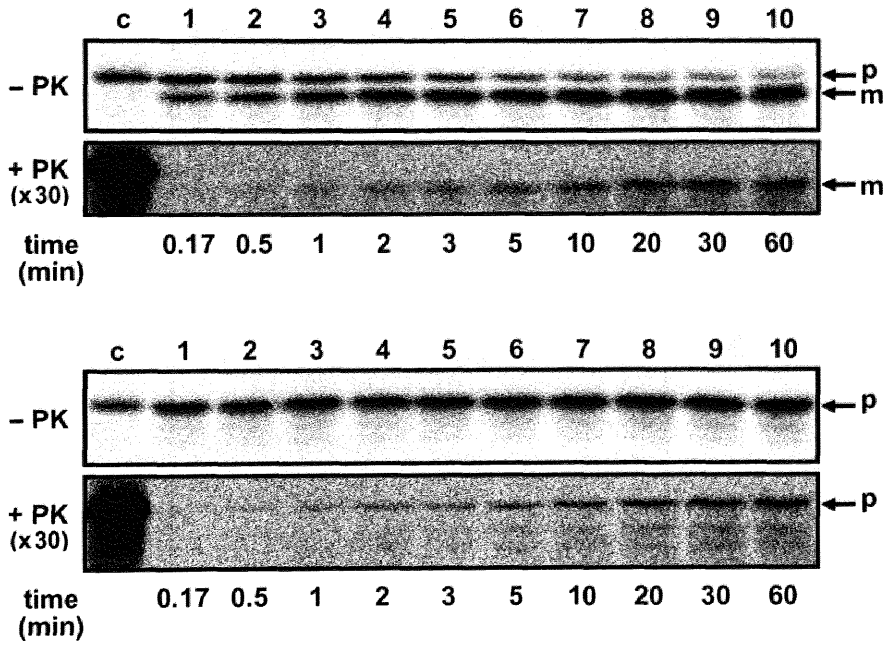

Figure 2-16. Tim50 precursor is slowly imported into mitochondria

Radiolabeled Tim50 precursor was incubated with isolated mitochondria for indicated times in the absence (upper panels) or presence (lower panels) of *o*-phenanthroline and EDTA. The samples were divided into halves, and one aliquot was kept on ice (-PK) and the other was treated with 100 μg/mg proteinase K for 20 min on ice (+PK). The mitochondria were reisolated and proteins were analyzed by SDS-PAGE and radioimaging. The intensities for "+PK" are enhanced 30-fold as compared with that for "-PK". p and m, precursor and mature forms of Tim50, respectively.

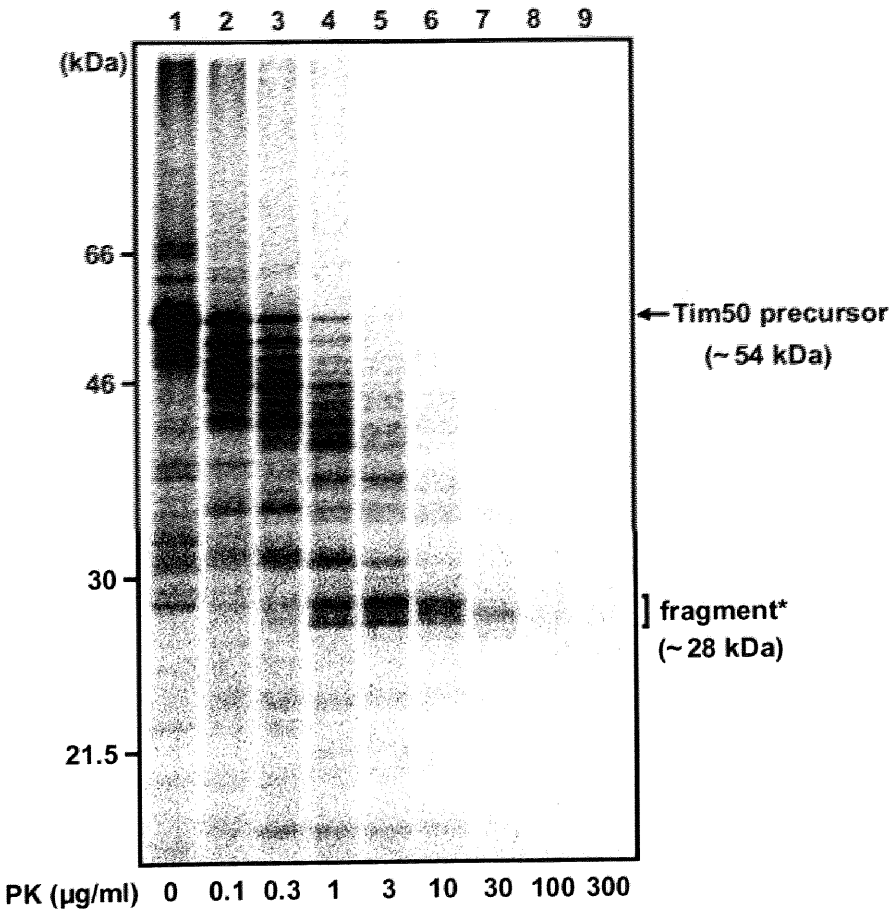

Figure 2-17. Tim50 precursor is partially folded

Radiolabeled Tim50 precursor was incubated with 0-300 μg/ml proteinase K in 250 mM sucrose, 1 mM EDTA, and 10 mM MOPS-KOH pH 7.2 for 15 min on ice and then precipitated with TCA. The samples were analyzed by SDS-PAGE and radioimaging. fragment*, protease-resistant fragment of Tim50 precursor.

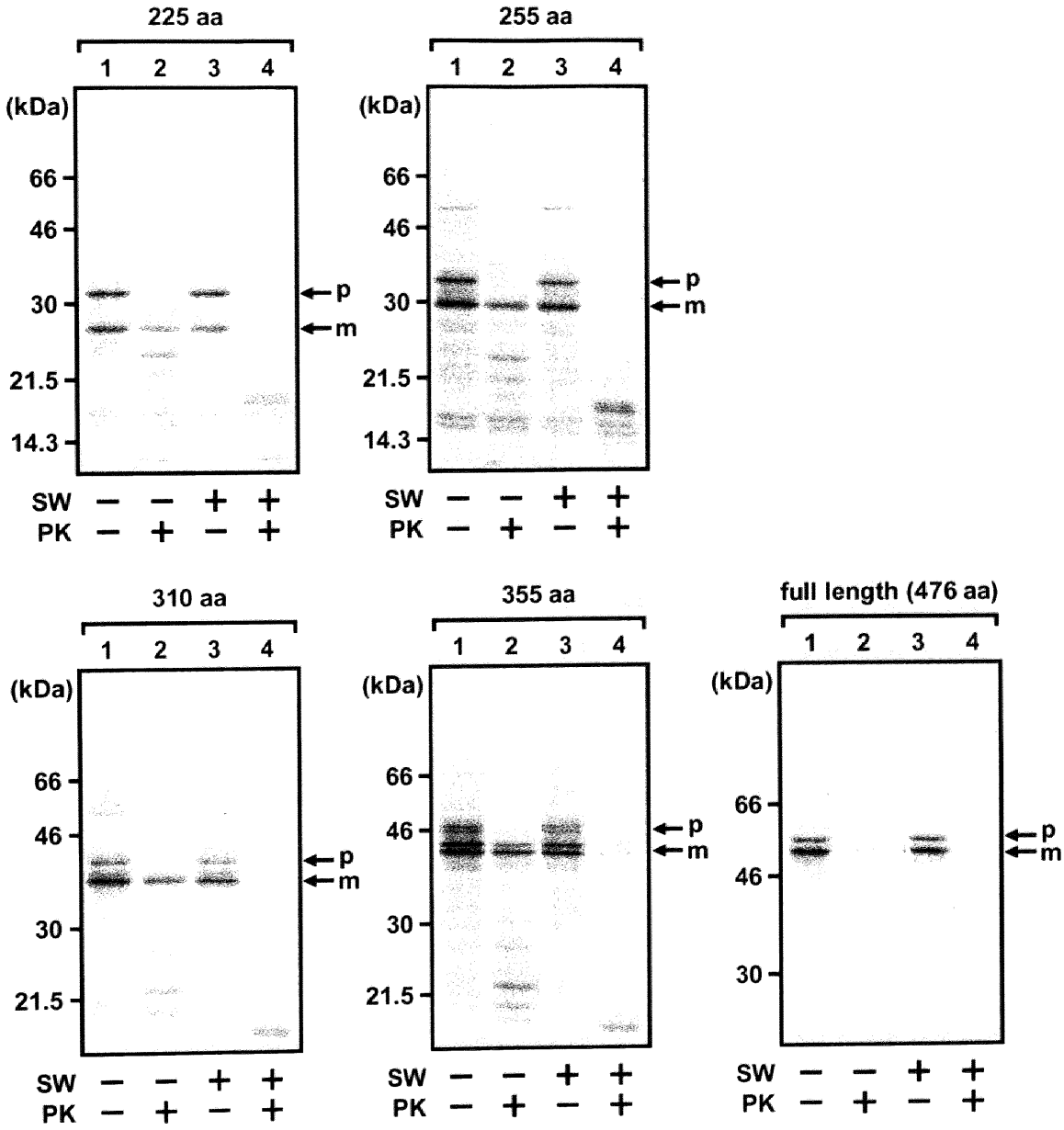

Figure 2-18. The C-terminally truncated Tim50 precursor, but not the full-length Tim50 precursor, is efficiently imported into mitochondria

Radiolabeled C-terminally truncated Tim50 precursors, which are consist of residues 1-225, residues 1-255, residues 1-310, or residues 1-355 of Tim50 precursor (225 aa, 255 aa, 310 aa, or 355 aa, respectively), and full-length Tim50 precursor (full length (476 aa)) were incubated with isolated mitochondria for 20 min at 30°C. The mitochondria were reisolated, converted to mitoplasts by osmotic swelling (lanes 1 and 2), and treated with 100 μg/mg proteinase K for 20 min on ice (lanes 2 and 4). The mitochondria and mitoplasts were reisolated and proteins were analyzed by SDS-PAGE and radioimaging. SW, osmotic swelling; PK, proteinase K treatment, p and m, precursor and mature forms of Tim50, respectively.

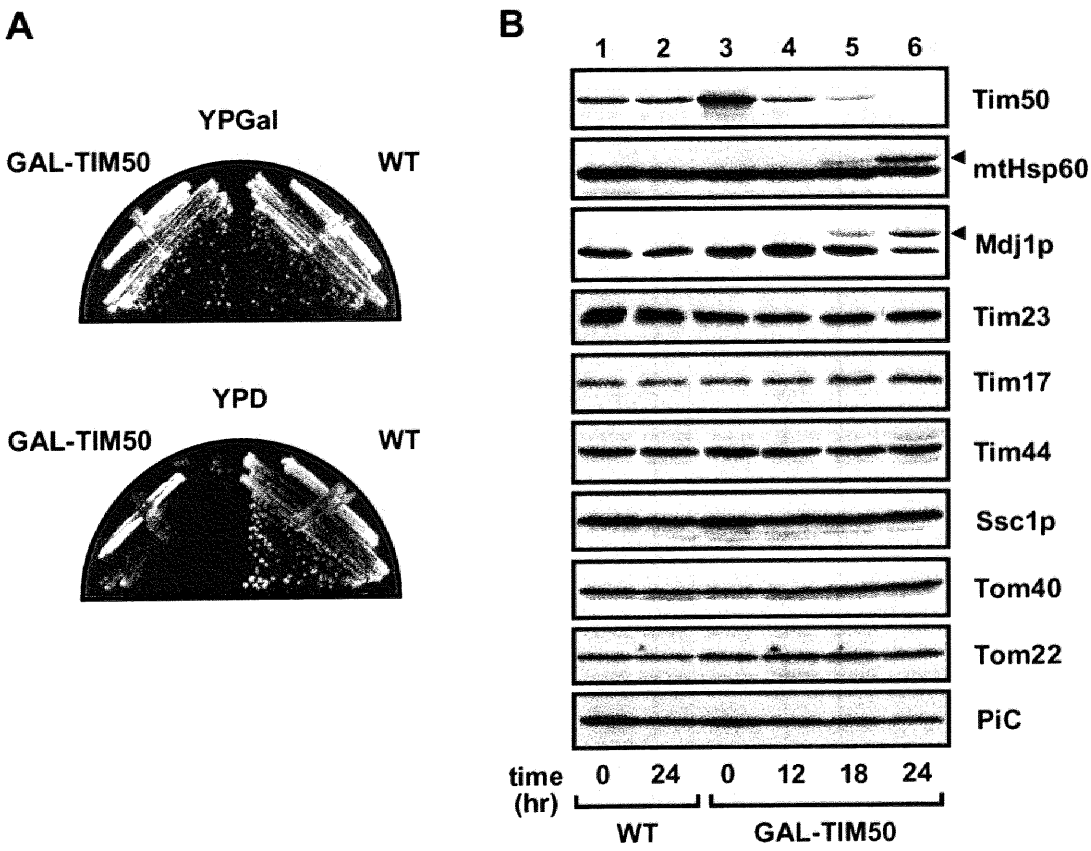

Figure 2-19. Depletion of Tim50 leads to accumulation of mitochondrial precursor proteins *in vivo*

(A) Yeast wild-type strain W303-1A (WT) and the GAL-TIM50 strain, in which the promoter of *TIM50* is replaced by the inducible *GAL7* promoter, were streaked onto galactose-containing medium (YPGal) and glucose-containing medium (YPD), and incubated at 23°C for 3 days and for 5 days, respectively. (B) Total lysates were prepared from yeast strains W303-1A (WT) and GAL-TIM50, which were grown at 23°C in YPGal, diluted, and then grown at 23°C in YPD for 0, 12, 18, and 24 hr. Total protein was isolated and analyzed by SDS-PAGE and immunoblotting with antibodies against the indicated proteins. The arrowheads indicate the accumulated precursor forms of mtHsp60 and Mdj1p.

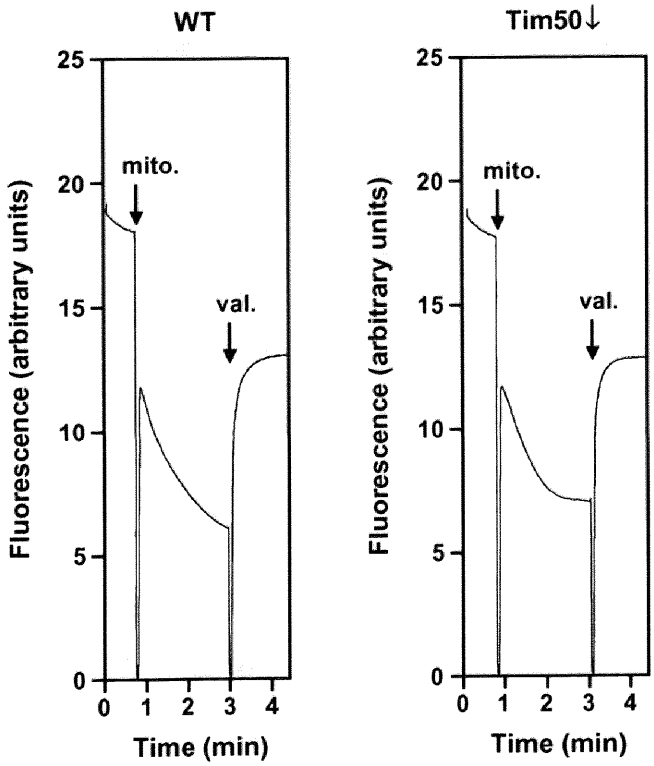

Figure 2-20. Tim50-depleted mitochondria generate the membrane potential

Mitochondria were isolated from yeast strains W303-1A (WT) and GAL-TIM50 (Tim50↓) after cultivation in glucose-containing medium for 12 hr at 30°C. The $\Delta\Psi$ of the isolated mitochondria was assessed by fluorescence quenching with the potential-sensitive dye $DiSC_3(5)$. The amount of Tim50 in Tim50↓ mitochondria was 19% of that of WT mitochondria (see Figure 2-28, lanes 3 and 5, Tim50). mito., addition of mitochondria; val., addition of valinomycin.

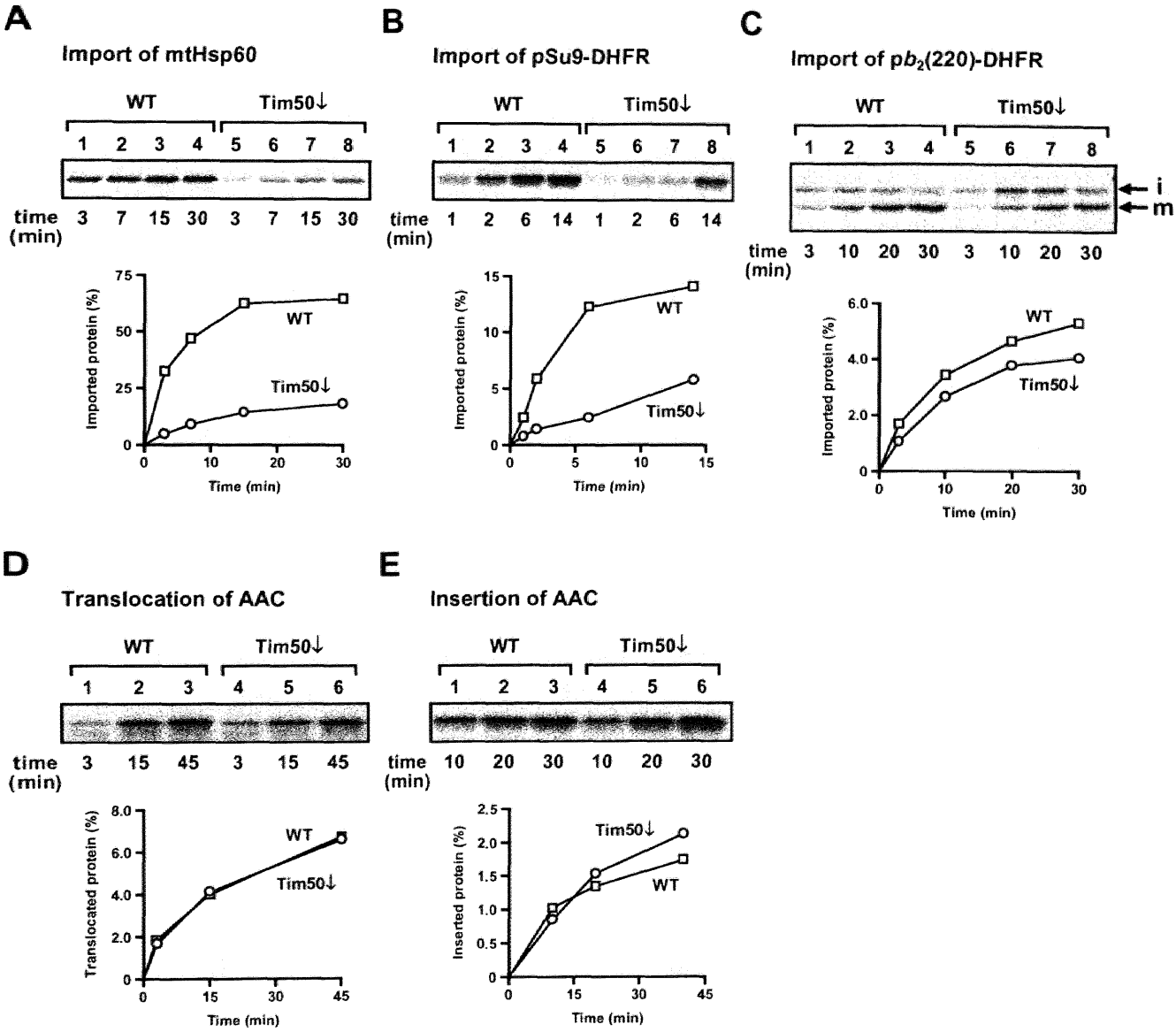

Figure 2-21. Depletion of Tim50 leads to retardation of the import of presequence-containing precursor proteins *in vitro*

Mitochondria were prepared as described in Figure 2-20. Radiolabeled mtHsp60 precursor (A), pSu9-DHFR (B), pb_2(220)-DHFR (C), and AAC (D and E) were incubated with WT mitochondria (squares) or Tim50↓ mitochondria (circles) at 23°C for indicated times. The mitochondria were treated with 100 μg/ml proteinase K for 20 min on ice to measure import of precursor proteins into mitochondria (A, B, and C) or translocation of AAC across the outer membrane (D), or the mitoplasts generated from the mitochondria were treated with 100 μg/ml proteinase K for 20 min on ice to measure insertion of AAC into the inner membrane (E). The samples were analyzed by SDS-PAGE and radioimaging. The amounts of radiolabeled proteins added to each sample are set to 100%. i and m, processing-intermediate and mature forms of pb_2(220)-DHFR, respectively.

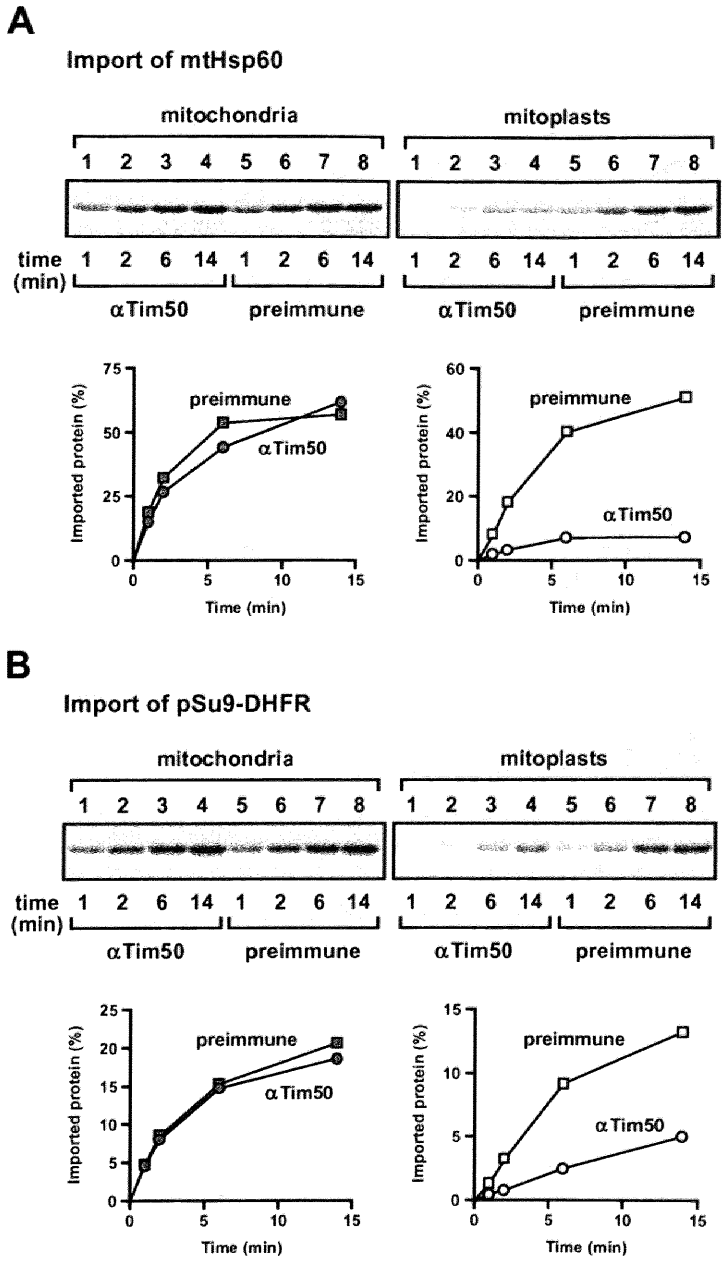

Figure 2-22. Import of precursor proteins into mitoplasts, but not into mitochondria, are blocked by anti-Tim50 antibodies

Mitochondria (filled symbols) and mitoplasts (blank symbols) (50 μg proteins) were preincubated with anti-Tim50 IgGs (αTim50; circles) or with IgGs prepared from the preimmune serum (preimmune; squares) (60 μg IgGs) for 30 min on ice. Radiolabeled mtHsp60 precursor (A) and pSu9-DHFR (B) were incubated with the IgG-treated mitochondria or mitoplasts at 23°C for indicated times. The mitochondria and mitoplasts were treated with 100 μg/ml proteinase K for 20 min on ice. The samples were analyzed by SDS-PAGE and radioimaging. The amounts of radiolabeled precursor proteins added to each sample are set to 100%.

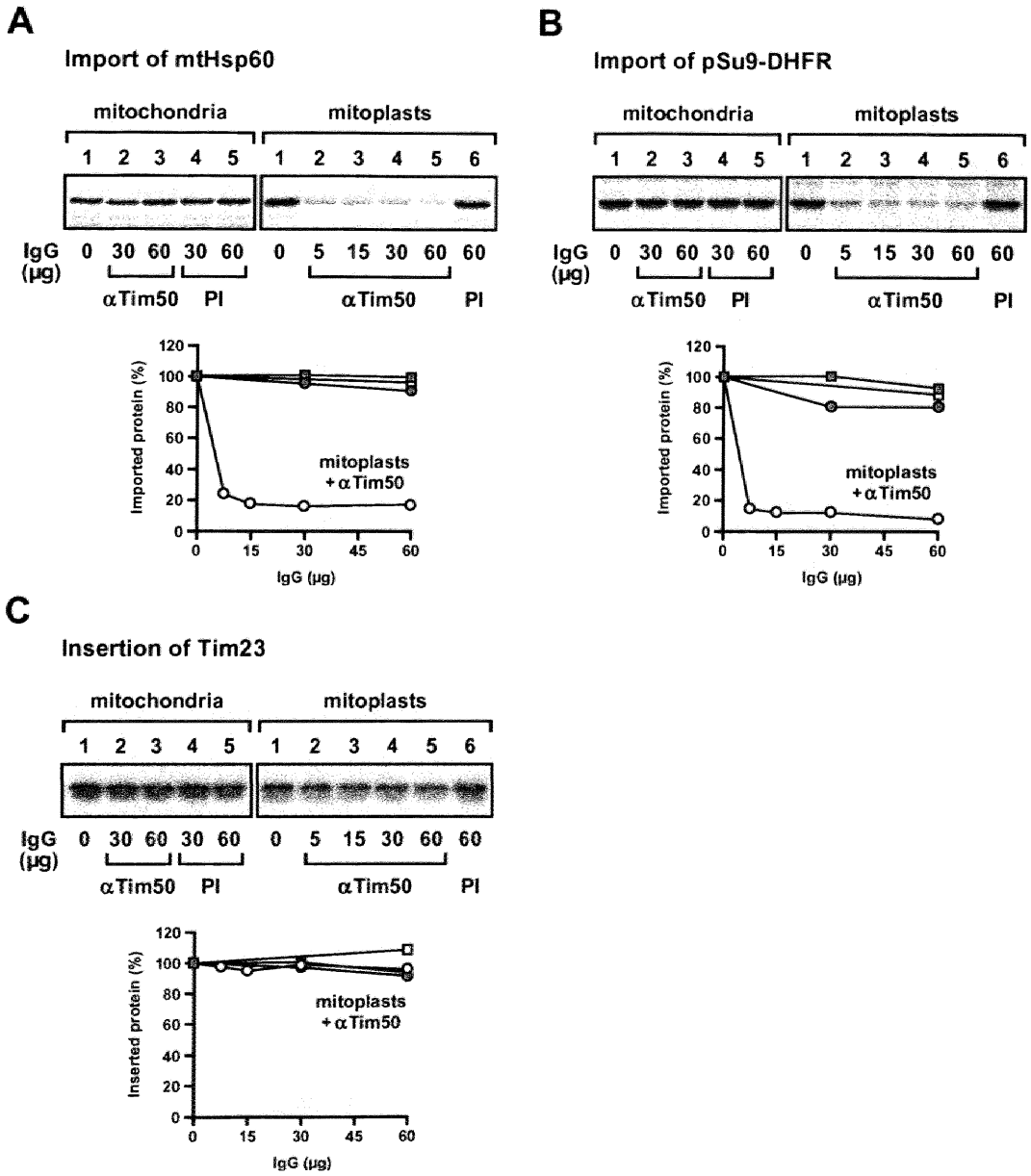

Figure 2-23. Import of presequence-containing precursor proteins, but not of presequence-less preproteins, are blocked by anti-Tim50 antibodies

Mitochondria (filled symbols) and mitoplasts (blank symbols) (50 µg proteins) were preincubated with indicated amounts of anti-Tim50 IgGs (αTim50; circles) or IgGs prepared from the preimmune serum (PI; squares) for 30 min on ice. Radiolabeled mtHsp60 precursor (A), pSu9-DHFR (B), and Tim23 (C) were incubated with the IgG-treated mitochondria or mitoplasts at 23°C for 6 min (A and B) or for 15 min (C). To measure import of mtHsp60 precursor and pSu9-DHFR (A and B), the mitochondria and mitoplasts were treated with 100 µg/ml proteinase K for 20 min on ice. To measure insertion of Tim23 (C), the mitochondria were converted to mitoplasts and the mitoplasts were treated with 250 µg/ml trypsin for 20 min on ice. The samples were analyzed by SDS-PAGE and radioimaging. For the insertion of Tim23, the trypsin-resistant fragment, which represent Tim23 inserted into the inner membrane, is shown. The amounts of radiolabeled proteins imported or inserted in a control sample without IgGs are set to 100%.

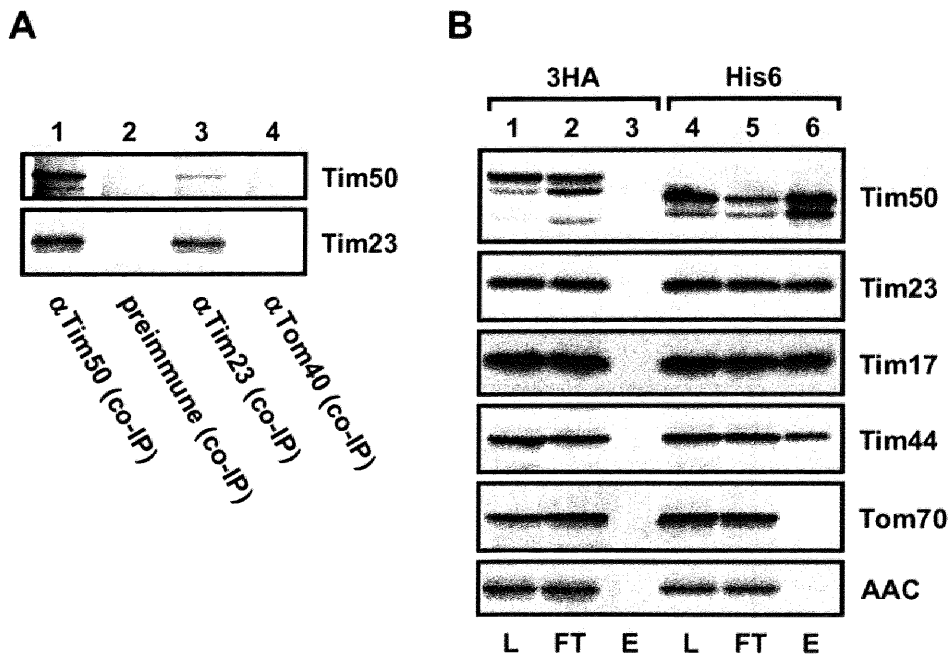

Figure 2-24. Tim50 is a subunit of the TIM23 complex

(A) Mitochondria were solubilized with 2% digitonin and subjected to co-immunoprecipitation using antibodies against Tim50 (αTim50 (co-IP)), Tim23 (αTim23 (co-IP)), and Tom40 (αTom40 (co-IP)) and using the preimmune serum (preimmune (co-IP)). Immunoprecipitates were analyzed by SDS-PAGE and immunoblotting with antibodies against Tim50 and Tim23.

(B) Mitochondria were prepared from yeast strains expressing Tim50-3HA (3HA) or Tim50-His6 (His6) instead of wild-type Tim50. The mitochondria were solubilized with 1% digitonin and incubated with the Ni-NTA resin, which was subsequently washed with 20 mM imidazole, and proteins bound to the resin were eluted with 250 mM imidazole. Proteins were analyzed by SDS-PAGE and immunoblotting with antibodies against the indicated proteins. Tim50 had slight degradation during the analysis. L, loaded sample; FT, flow-through fraction; E, eluted fraction.

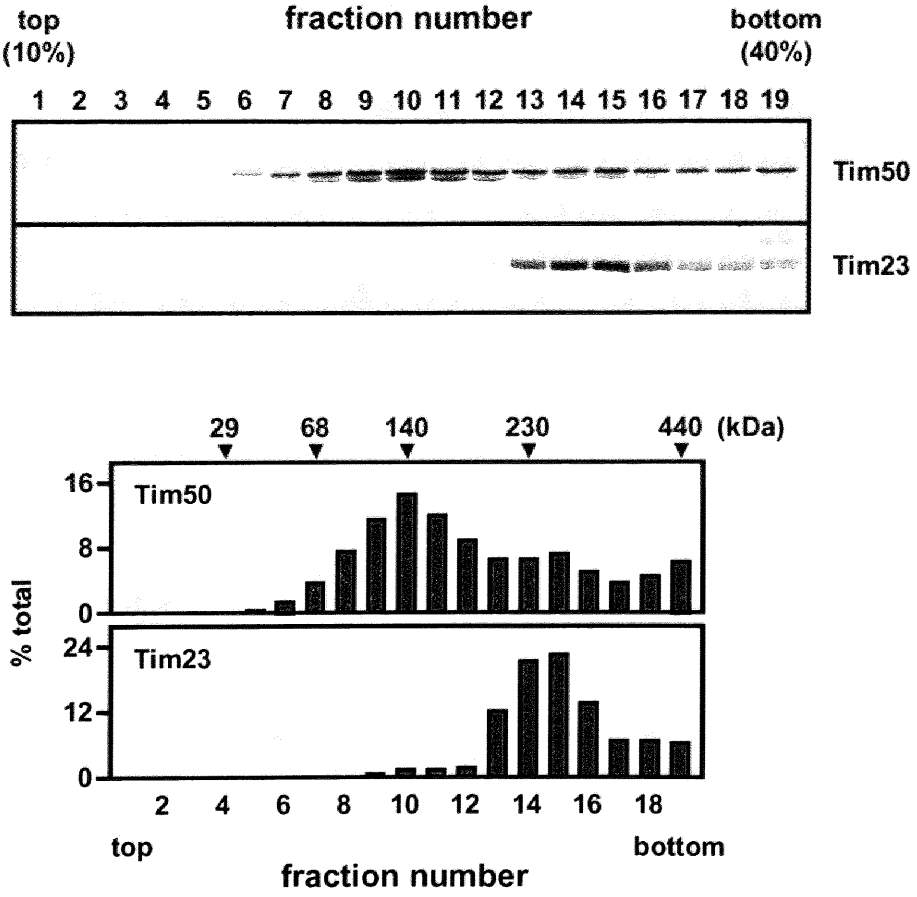

Figure 2-25. Tim50 partly associates with the TIM23 complex

Mitochondria were solubilized with 1% digitonin, layered onto 10-40% linear glycerol gradient, and centrifugated at 200,000 × *g* for 15 hr at 4°C. After centrifugation, fractions were collected from the top and analyzed by SDS-PAGE and immunoblotting with antibodies against Tim50 and Tim23. Numbers indicate fractions (from top to bottom). Vertical arrowheads show the positions of carbonic anhydrase (29 kDa), BSA (68 kDa), alcohol dehydrogenase (140 kDa), catalase (230 kDa), and apoferritin (440 kDa).

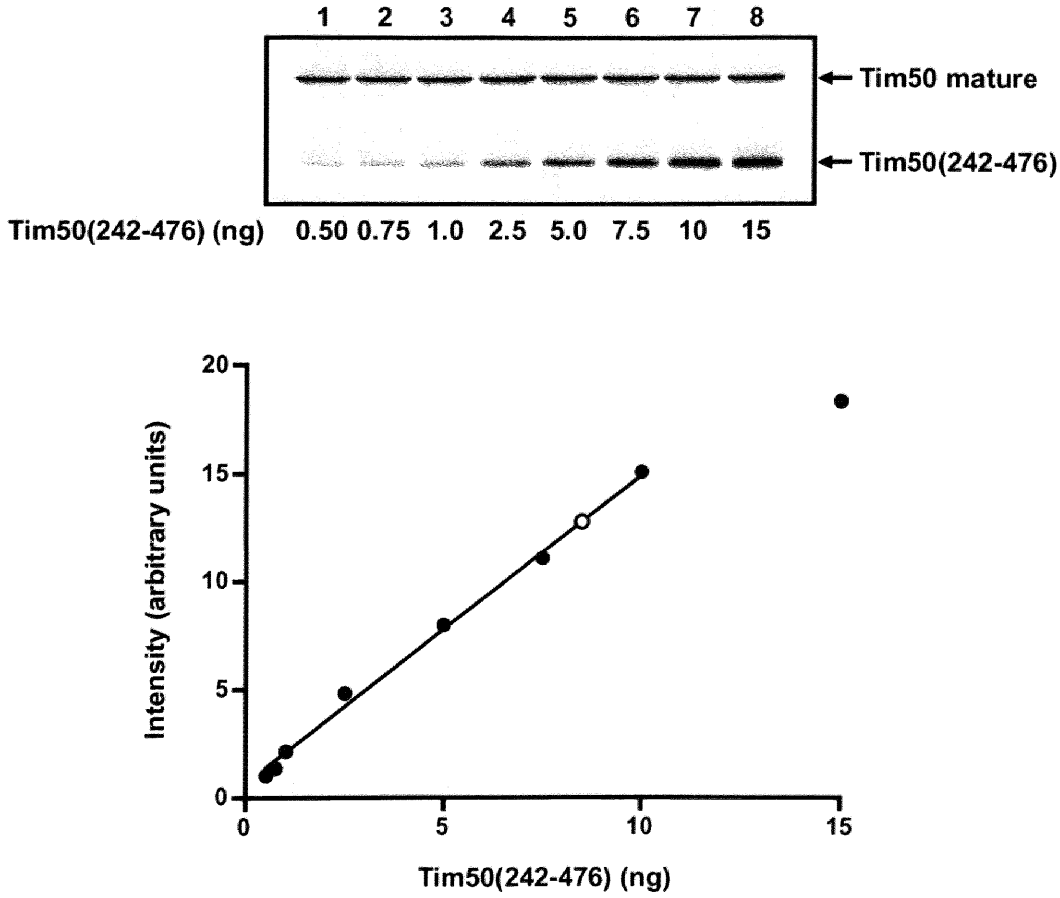

Figure 2-26. Mitochondria contain ~30 pmol of Tim50 per mg of mitochondrial protein

Together with isolated yeast mitochondria (10 μg protein each), indicated amounts of the C-terminal segment (residues 242-476) of Tim50 (Tim50(242-476)) purified from *E. coli* cells were subjected to SDS-PAGE and analyzed by immunoblotting with anti-Tim50 antibodies. The intensity for 0.50 ng of Tim50(242-476) is set to 1 unit. Blank circle indicates the intensity for endogenous mature form of Tim50 in 10 μg of yeast mitochondrial proteins.

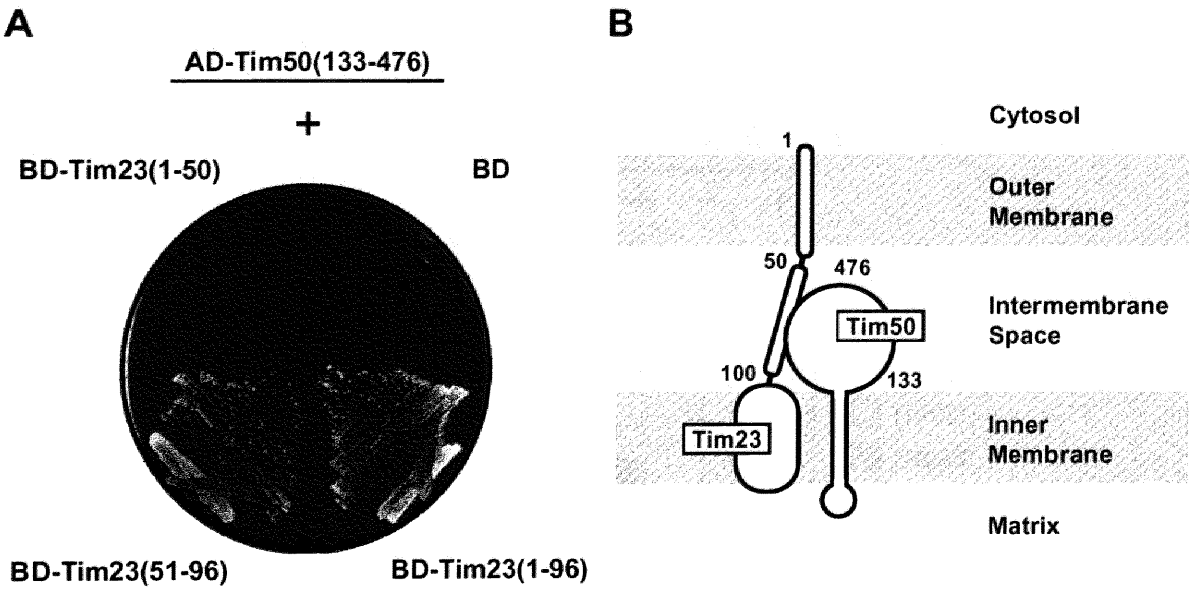

Figure 2-27. The intermembrane-space domain of Tim50 directly interacts with the intermembrane-space domain of Tim23

(A) The IMS domain (residues 133-476) of Tim50 expressed as a fusion to the Gal4p activator domain (AD-Tim50(133-476)) was assayed for interactions with residues 1-50, residues 51-96, and residues 1-96 of Tim23 as fusions to the Gal4p DNA binding domain (BD-Tim23(1-50), BD-Tim23(51-96), and BD-Tim23(1-96), respectively) and with the Gal4p DNA binding domain (BD) as a control in yeast two-hybrid analysis. The plasmids for the BD fusions were individually co-transformed with the plasmid for AD-Tim50(133-476) into yeast strain PJ69-4A and incubated on minimal SD medium lacking adenine at 30°C for 3 days.
(B) Deduced topology of Tim50 and Tim23 is schematically outlined.

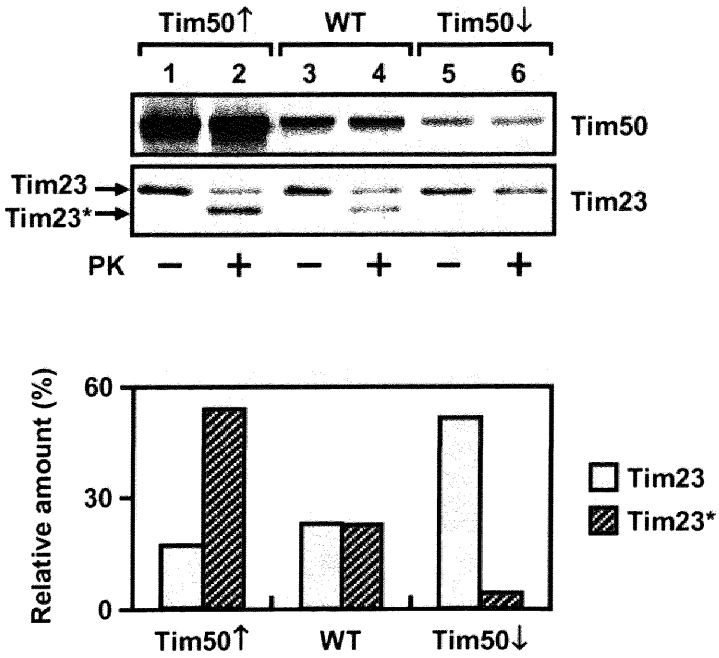

Figure 2-28. Tim50 affects the protease sensitivity of Tim23

Yeast strain GAL-TIM50 was grown in galactose-containing medium or glucose-containing medium for 12 hr at 30°C to prepare mitochondria overexpressing Tim50 (Tim50↑) or those depleted of Tim50 (Tim50↓), respectively. Wild-type mitochondria (WT) were prepared from yeast strain W303-1A grown in glucose-containing medium for 12 hr at 30°C. The mitochondria were treated with 500 μg/ml proteinase K in 250 mM sucrose, 10 mM MOPS-KOH pH 7.2, and 80 mM KCl for 20 min on ice (lanes 2, 4, and 6). The mitochondria were reisolated and proteins were analyzed by SDS-PAGE and immunoblotting with antibodies against Tim50 and Tim23. The amounts of Tim23 in lanes 1, 3, and 5 are set to 100% for the those of Tim23 and Tim23* in lanes 2, 4, and 6, respectively. PK, proteinase K treatment; Tim23*, a proteolytic fragment of Tim23 in mitochondria.

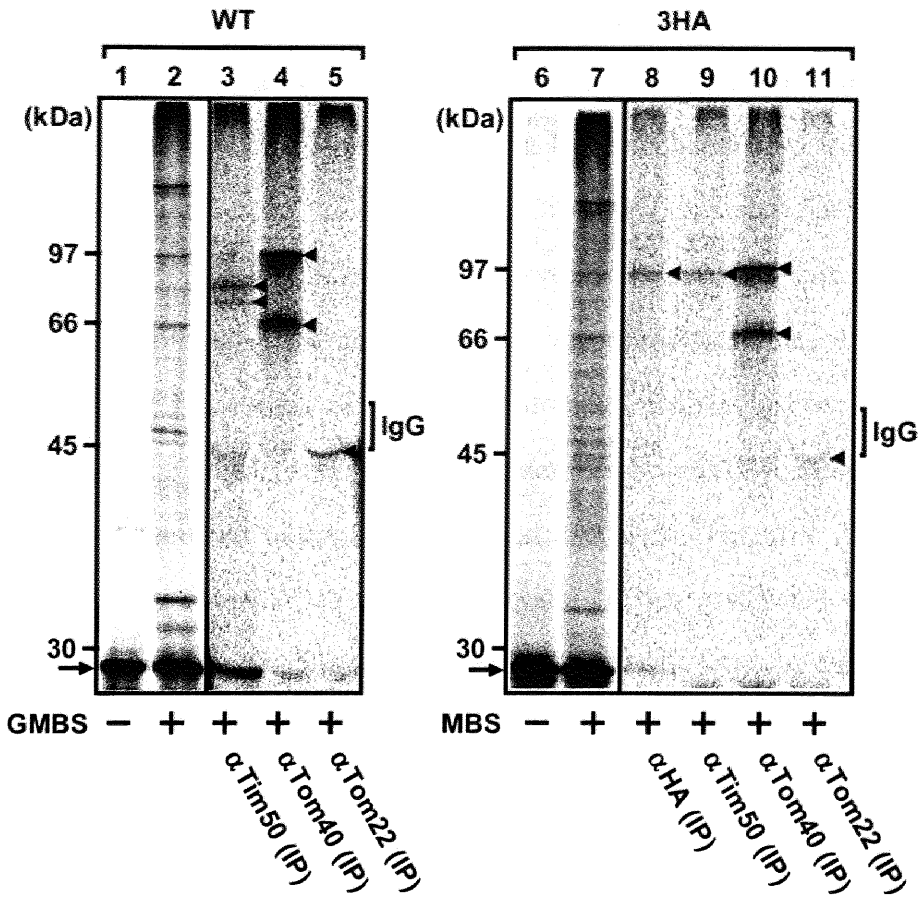

Figure 2-29. The translocation intermediate of pSu9-DHFR lodged in the TOM channel is crosslinked to Tim50

Mitochondria were prepared from yeast wild-type strain (WT) and yeast strain expressing Tim50-3HA instead of wild-type Tim50 (3HA). To generate the translocation intermediate lodged in the TOM channel, radiolabeled pSu9-DHFR was incubated with the mitochondria for 10 min at 30°C in the presence of CCCP. The mitochondria carrying wild-type Tim50 (left panel) and those carrying Tim50-3HA (right panel) were reisolated and subjected to crosslinking with 200 μM GMBS and 200 μM MBS, respectively, for 60 min on ice. After quenching the crosslinking reaction, the mitochondria were reisolated, solubilized with 1% SDS, and subjected to immunoprecipitation with antibodies against Tim50 (αTim50 (IP)), Tom40 (αTom40 (IP)), and Tom22 (αTom22 (IP)) and with anti-HA monoclonal antibody (αHA (IP)). The immunoprecipitates were analyzed by SDS-PAGE and radioimaging. The intensities for lanes 3-5 and for lanes 8-10 are 25-fold and 40-fold higher than those for lanes 1-2 and for lanes 6-7, respectively. Arrowheads indicate the identified crosslinked products, and arrows pSu9-DHFR.

2-4. Discussion

In the present study, I identified a novel protein Tim50 in yeast *S. cerevisiae* as a crosslinked partner of the translocation intermediate anchored to the mitochondrial inner membrane. Tim50 is an integral inner-membrane protein and exposes a large C-terminal domain to the IMS, which interacts with the N-terminal IMS segment of Tim23. Depletion of Tim50 led to accumulation of precursor forms of mitochondrial proteins *in vivo* and exhibited defects in the import of presequence-containing precursor proteins *in vitro*. Besides, anti-Tim50 antibodies blocked the import of presequence-containing precursor proteins, but not of presequence-less preproteins, into mitoplasts. These results indicate that Tim50 is a key component of the TIM23 complex that is directly involved in the early step of the protein translocation across the inner membrane. Glycerol density gradient centrifugation of solubilized mitochondria showed that, while Tim50 is a subunit of the TIM23 complex, only one third of the Tim50 molecules are associated with the TIM23 complex and the rest of the Tim50 molecules forms a pool of ~140-kDa complex, which is distinct from the TIM23 complex. The interaction of Tim50 with the TIM23 complex appears to be dynamic.

Recently, Tim50 was also identified in *N. crassa* as an additional protein purified with the TIM23 complex (35). Tim50 in *N. crassa* consists of 540 amino-acid residues, possesses a mitochondrial presequence (residues 1-37), spans the inner membrane with a single transmembrane segment (residues 171-191), and exposes a large C-terminal domain to the IMS, as yeast Tim50 does. While *N. crassa* Tim50 is a functional subunit of the TIM23 complex, only a fraction of the Tim50 molecules were found in association with the TIM23 complex (35). The molar ratio of Tim50:Tim23:Tim17 was estimated to be ~2:1:1 in mitochondria and ~0.3:1:1 in the purified TIM23 complex in *N. crassa*. These features of *N. crassa* Tim50 are similar to those of yeast Tim50 described in the present study.

What is the role of Tim50 in protein import into mitochondria? Tim50 is the only

subunit of the TIM23 complex that exposes its largest domain to the IMS and could be dynamically associated with the TIM23 complex. Since this IMS-exposed C-terminal domain is tightly folded and highly conserved in evolution, it may well be a functional region of Tim50. The IMS domain of Tim50 also contains a coiled-coil segment, which can mediate a protein-protein interaction. Indeed, Tim50, most likely via its IMS domain, was efficiently crosslinked to the translocation intermediate lodged in the TOM channel in the absence of $\Delta\Psi$. This strongly suggests that Tim50 is involved in the transfer of precursor proteins from the outlet of the TOM channel to the TIM23 complex. Besides, the recent studies showed that Tim50 is crosslinked to the translocating precursor protein, which spans both the TOM and TIM23 complexes to generate the TOM-TIM23-preprotein supercomplex (35, 36). Furthermore, it was reported that Tim50 is strictly required for generation, but not for stabilization, of the TOM-TIM23-preprotein supercomplex (37). When the supercomplex is generated, the bulk of Tim50 is included in the supercomplex but easily released as it is not necessary for the stable interaction between the precursor protein and the TOM and TIM23 complexes (37). These recent findings would also support my view for the role of Tim50 in linking the TOM complex to the TIM23 complex.

Previously, the IMS domain of Tom22, which contributes to a presequence-binding site, and the extreme N-terminal segment of Tim23, which is integrated into the outer membrane, have been suggested to facilitate the transfer of precursor proteins from the TOM complex to the TIM23 complex. The mitochondria containing a mutant Tom22 that lacks its IMS domain exhibit no defect in the accumulation of the translocation intermediate in the absence of $\Delta\Psi$, but impairs the chase of the intermediate into the matrix after regeneration of $\Delta\Psi$ (32, 38, 39). In addition, this IMS domain of Tom22 is crucial for generation of the TOM-TIM23-preprotein supercomplex (37). The mitochondria containing a mutant Tim23 that lacks its N-terminal segment (residues 1-50) exhibit defects in protein import into mitochondria, but not into the mitoplasts (31), although another group

failed to confirm these results (37). Thus, the N-terminal segment of Tim23 stimulates the transfer of precursor proteins from the TOM complex to the TIM23 complex, probably by tethering the TIM23 complex to the outer membrane. Taken together, I propose here that Tim50, in cooperation with the IMS domain of Tom22, links protein translocation across the outer membrane and that across the inner membrane, in the following manner. An incoming precursor protein, which traverses the outer membrane, binds to the *trans* site of the TOM complex on the IMS side of the outer membrane and/or the IMS domain of Tim50 in the IMS. In this state, Tim50 may possibly be separated from the TIM23 complex and present in the ~140-kDa complex in which Tim50 forms a homodimer via its C-terminal coiled-coil region. Then, the precursor protein is delivered from Tim50 to the TIM23 complex by association of its IMS domain with the IMS segment (residues 51-96) of Tim23. Finally, the presequence of the precursor protein, which was bound by the IMS segment of Tim23, is translocated across the inner membrane with the aid of $\Delta\Psi$. Since a coiled-coil dimer can bind to another coiled-coil segment to exchange its dimeric pair (40, 41) and the IMS segment of Tim23 also forms a coiled-coil dimer (42), the IMS domain of Tim50 could perhaps open the Tim23 channel or dissociate the Tim23 dimer by changing its coiled-coil partner to Tim23. This hypothesis should be addressed in future studies. In particular, which forms of Tim50 (~250-kDa form with the TIM23 complex or ~140-kDa form without the TIM23 complex) is crosslinked with the translocation intermediate accumulated at the outer membrane and whether Tim50 functions as a pore-opening factor for the Tim23 channel are the questions to be answered.

Although Tim50 is not essential for stabilization of the TOM-TIM23-preprotein supercomplex, the bulk of Tim50 is present in the supercomplex (37). Why is Tim50 still enriched in the supercomplex? Tim50 is crosslinked to the processing-intermediate form of translocating pb_2(220)-DHFR, not the mature form, through just downstream of the IMS-sorting signal of the Cytb_2 part. Therefore, it is possible that Tim50 is responsible for

the sorting function, or, more specifically, the recognition of the IMS-sorting signal of the Cytb_2 precursor as well as for protein translocation across the inner membrane. Such a role was previously assigned to Tim23 and Tim11. Mitochondria containing a mutant Tim23 affect the sorting of the Cytb_2 precursor with an altered sorting signal (43). Tim11 was efficiently crosslinked to the IMS-sorting signal part of the Cytb_2 precursor (44). However, since Tim11 was found to be a subunit of F_1F_o-ATPase and was not included in the TIM23 complex (45), it may not be involved in intramitochondrial sorting. The possible roles of Tim50 and Tim23 in sorting proteins to the IMS, e.g., recognition of the IMS sorting signal and discharge of the IMS proteins from the TIM23 complex, will be an essential subject of future studies.

2-5. References

1) Daum, G., Gasser, S. M., and Schatz, G. (1982) Import of proteins into mitochondria. Energy-dependent, two-step processing of the intermembrane space enzyme cytochrome b_2 by isolated yeast mitochondria. *J. Biol. Chem.*, **257**, 13075-13080.

2) Esaki, M., Kanamori, T., Nishikawa, S., and Endo, T. (1999) Two distinct mechanisms drive protein translocation across the mitochondrial outer membrane in the late step of the cytochrome b_2 import pathway. *Proc. Natl. Acad. Sci. USA*, **96**, 11770-11775.

3) Geli, V., Yang, M. J., Suda, K., Lustig, A., and Schatz, G. (1990) The MAS-encoded processing protease of yeast mitochondria. Overproduction and characterization of its two nonidentical subunits. *J. Biol. Chem.*, **265**, 19216-19222.

4) Schneider, A., Behrens, M., Scherer, P., Pratje, E., Michaelis, G., and Schatz, G. (1991) Inner membrane protease I, an enzyme mediating intramitochondrial protein sorting in yeast. *EMBO J.*, **10**, 247-254.

5) Rospert, S., Müller, S., Schatz, G., and Glick, B. S. (1994) Fusion proteins containing the cytochrome b_2 presequence are sorted to the mitochondrial intermembrane space independently of hsp60. *J. Biol. Chem.*, **269**, 17279-17288.

6) Gruhler, A., Ono, H., Guiard, B., Neupert, W., and Stuart, R. A. (1995) A novel intermediate on the import pathway of cytochrome b_2 into mitochondria: evidence for conservative sorting. *EMBO J.*, **14**, 1349-1359.

7) Kanamori, T., Nishikawa, S., Shin, I., Schultz, P. G., and Endo, T. (1997) Probing the environment along the protein import pathways in yeast mitochondria by site-specific photocrosslinking. *Proc. Natl. Acad. Sci. USA*, **94**, 485-490.

8) Kitada, K., Yamaguchi, E., and Arisawa, M. (1995) Cloning of the *Candida glabrata TRP1* and *HIS3* genes, and construction of their disruptant strains by sequential integrative transformation. *Gene*, **165**, 203-206.

9) Huxley, C., Green, E. D., and Dunham, I. (1990) Rapid assessment of *S. cerevisiae*

mating type by PCR. *Trends Genet.*, **6**, 236.

10) Sato, M. H. and Wada, Y. (1997) Universal template plasmid for introduction of the triple-HA epitope sequence into cloned genes. *Biotechniques*, **23**, 254-256.

11) Kunkel, T. A. (1985) Rapid and efficient site-specific mutagenesis without phenotypic selection. *Proc. Natl. Acad. Sci. USA*, **82**, 488-492.

12) Kunkel, T. A., Roberts, J. D., and Zakour, R. A. (1987) Rapid and efficient site-specific mutagenesis without phenotypic selection. *Methods Enzymol.*, **154**, 367-382.

13) Sikorski, R. S. and Hieter, P. (1989) A system of shuttle vectors and yeast host strains designed for efficient manipulation of DNA in *Saccharomyces cerevisiae*. *Genetics*, **122**, 19-27.

14) Rose, M. D., Winston, F., and Hieter, P. (1990) *Methods in Yeast Genetics: A Laboratory Course Manual.* (Cold Spring Harbor Laboratry Press, Cold Spring Harbor, NY).

15) James, P., Halladay, J., and Craig, E. A. (1996) Genomic libraries and a host strain designed for highly efficient two-hybrid selection in yeast. *Genetics*, **144**, 1425-1436.

16) Daum, G., Böhni, P. C., and Schatz, G. (1982) Import of proteins into mitochondria. Cytochrome b_2 and cytochrome *c* peroxidase are located in the intermembrane space of yeast mitochondria. *J. Biol. Chem.*, **257**, 13028-13033.

17) Abe, Y., Odaka, M., Inagaki, F., Lax, I., Schlessinger, J., and Kohda, D. (1988) Disulfide bond structure of human epidermal growth factor receptor. *J. Biol. Chem.*, **273**, 11150-11157.

18) Kawai, A., Nishikawa, S., Hirata, A., and Endo, T. (2001) Loss of the mitochondrial Hsp70 functions causes aggregation of mitochondria in yeast cells. *J. Cell Sci.*, **114**, 3565-3574.

19) Jackson, R. J. and Hunt, T. (1983) Preparation and use of nuclease-treated rabbit

reticulocyte lysates for the translation of eukaryotic messenger RNA. *Methods Enzymol.*, **96**, 50-74.

20) Stueber, D., Ibrahimi, I., Cutler, D., Dobberstein, B., and Bujard, H. (1984) A novel *in vitro* transcription-translation system: accurate and efficient synthesis of single proteins from cloned DNA sequences. *EMBO J.*, **3**, 3143-3148.

21) Hurt, E. C., Pesold-Hurt, B., and Schatz, G. (1984) The amino-terminal region of an imported mitochondrial precursor polypeptide can direct cytoplasmic dihydrofolate reductase into the mitochondrial matrix. *EMBO J.*, **3**, 3149-3156.

22) Claros, M. G. and Vincens, P. (1996) Computational method to predict mitochondrially imported proteins and their targeting sequences. *Eur. J. Biochem.*, **241**, 779-786.

23) Pfanner, N., Douglas, M. G., Endo, T., Hoogenraad, N. J., Jensen, R. E., Meijer, M., Neupert, W., Schatz, G., Schmitz, U. K., and Shore, G. C. (1996) Uniform nomenclature for the protein transport machinery of the mitochondrial membranes. *Trends Biochem. Sci.*, **21**, 51-52.

24) Kobor, M. S., Archambault, J., Lester, W., Holstege, F. C., Gileadi, O., Jansma, D. B., Jennings, E. G., Kouyoumdjian, F., Davidson, A. R., Young, R. A., and Greenblatt, J. (1999) An unusual eukaryotic protein phosphatase required for transcription by RNA polymerase II and CTD dephosphorylation in *S. cerevisiae*. *Mol. Cell*, **4**, 55-62.

25) Siniossoglou, S., Santos-Rosa, H., Rappsilber, J., Mann, M., and Hurt, E. (1998) A novel complex of membrane proteins required for formation of a spherical nucleus. *EMBO J.*, **17**, 6449-6464.

26) Siniossoglou, S., Hurt, E. C., and Pelham, H. R. B. (2000) Psr1p/Psr2p, two plasma membrane phosphatases with an essential D*X*D*X*(T/V) motif required for sodium stress response in yeast. *J. Biol. Chem.*, **275**, 19352-19360.

27) Collet, J.-F., Stroobant, V., Pirard, M., Delpierre, G., and Van Schaftingen, E. (1998) A

new class of phosphotransferases phosphorylated on an aspartate residue in an amino-terminal D*X*D*X*(T/V) motif. *J. Biol. Chem.*, **273**, 14107-14112.

28) Diehn, M., Eisen, M. B., Botstein, D., and Brown, P. O. (2000) Large-scale identification of secreted and membrane-associated gene products using DNA microarrays. *Nat. Genet.*, **25**, 58-62.

29) Dekker, P. J. T., Martin, F., Maarse, A. C., Bömer, U., Müller, H., Guiard, B., Meijer, M., Rassow, J., and Pfanner, N. (1997) The Tim core complex defines the number of mitochondrial translocation contact sites and can hold arrested preproteins in the absence of matrix Hsp70-Tim44. *EMBO J.*, **16**, 5408-5419.

30) Sirrenberg, C., Endres, M., Becker, K., Bauer, M. F., Walther, E., Neupert, W., and Brunner, M. (1997) Functional cooperation and stoichiometry of protein translocases of the outer and inner membranes of mitochondria. *J. Biol. Chem.*, **272**, 29963-29966.

31) Donzeau, M., Káldi, K., Adam, A., Paschen, S., Wanner, G., Guiard, B., Bauer, M. F., Neupert, W., and Brunner, M. (2000) Tim23 links the inner and outer mitochondrial membranes. *Cell*, **101**, 401-412.

32) Kanamori, T., Nishikawa, S., Nakai, M., Shin, I., Schultz, P. G., and Endo, T. (1999) Uncoupling of transfer of the presequence and unfolding of the mature domain in precursor translocation across the mitochondrial outer membrane. *Proc. Natl. Acad. Sci. USA*, **96**, 3634-3639.

33) Kyte, J. and Doolittle, R. F. (1982) A simple method for displaying the hydropathic character of a protein. *J. Mol. Biol.*, **157**, 105-132.

34) Thompson, J. D., Gibson, T. J., Plewniak, F., Jeanmougin, F., and Higgins, D. G. (1997) The CLUSTAL_X windows interface: flexible strategies for multiple sequence alignment aided by quality analysis tools. *Nucleic Acids Res.*, **25**, 4876-4882.

35) Mokranjac, D., Paschen, S. A., Kozany, C., Prokisch, H., Hoppins, S. C., Nargang, F. E., Neupert, W., and Hell, K. (2003) Tim50, a novel component of the TIM23

preprotein translocase of mitochondria. *EMBO J.*, **22**, 816-825.

36) Geissler, A., Chacinska, A., Truscott, K. N., Wiedemann, N., Brandner, K., Sickmann, A., Meyer, H. E., Meisinger, C., Pfanner, N., and Rehling, P. (2002) The mitochondrial presequence translocase: an essential role of Tim50 in directing preproteins to the import channel. *Cell*, **111**, 507-518.

37) Chacinska, A., Rehling, P., Guiard, B., Frazier, A. E., Schulze-Specking, A., Pfanner, N., Voos, W., and Meisinger, C. (2003) Mitochondrial translocation contact sites: separation of dynamic and stabilizing elements in formation of a TOM-TIM-preprotein supercomplex. *EMBO J.*, **22**, 5370-5381.

38) Court, D. A., Nargang, F. E., Steiner, H., Hodges, R. S., Neupert, W., and Lill, R. (1996) Role of the intermembrane-space domain of the preprotein receptor Tom22 in protein import into mitochondria. *Mol. Cell. Biol.*, **16**, 4035-4042.

39) Moczko, M., Bömer, U., Kübrich, M., Zufall, N., Hönlinger, A., and Pfanner, N. (1997) The intermembrane space domain of mitochondrial Tom22 functions as a *trans* binding site for preproteins with N-terminal targeting sequences. *Mol. Cell. Biol.*, **17**, 6574-6584.

40) Amati, B., Brooks, M. W., Levy, N., Littlewood, T. D., Evan, G. I., and Land, H. (1993) Oncogenic activity of the c-Myc protein requires dimerization with Max. *Cell*, **72**, 233-245.

41) Carr, C. M. and Kim, P. S. (1993) A spring-loaded mechanism for the conformational change of influenza hemagglutinin. *Cell*, **73**, 823-832.

42) Bauer, M. F., Sirrenberg, C., Neupert, W., and Brunner, M. (1996) Role of Tim23 as voltage sensor and presequence receptor in protein import into mitochondria. *Cell*, **87**, 33-41.

43) Bömer, U., Meijer, M., Guiard, B., Dietmeier, K., Pfanner, N., and Rassow, J. (1997) The sorting route of cytochrome b_2 branches from the general mitochondrial import

pathway at the preprotein translocase of the inner membrane. *J. Biol. Chem.*, **272**, 30439-30446.

44) Tokatlidis, K., Junne, T., Moes, S., Schatz, G., Glick, B. S., and Kronidou, N. (1996) Translocation arrest of an intramitochondrial sorting signal next to Tim11 at the inner-membrane import site. *Nature*, **384**, 585-588.

45) Arnold, I., Bauer, M. F., Brunner, M., Neupert, W., and Stuart, R. A. (1997) Yeast mitochondrial F_1F_o-ATPase: the novel subunit e is identical to Tim11. *FEBS Lett.*, **411**, 195-200.